Synthesis, molecular docking and biochemical analysis of aminoalkylated naphthalene-based chalcones as acetylcholinesterase inhibitors

Ghadah Aljohani, Adeeb Al-Sheikh Ali, Shaya Y. Alraqa, Syazwani Itri Amran & Norazah Basar

JTUSCI

J of Taibah University for Science Journal

Taylor & Francis
Taylor & Francis Group

RESEARCH ARTICLE

OPEN ACCESS

Check for updates

Synthesis, molecular docking and biochemical analysis of aminoalkylated naphthalene-based chalcones as acetylcholinesterase inhibitors

Ghadah Aljohani [a,b], Adeeb Al-Sheikh Ali [a], Shaya Y. Alraqa [a], Syazwani Itri Amran [c] and Norazah Basar [b]

[a]Chemistry Department, College of Science, Taibah University, Al-Madinah Al Munawarah, Kingdom of Saudi Arabia; [b]Department of Chemistry, Faculty of Science, Universiti Teknologi Malaysia Johor Bahru, Malaysia; [c]Department of Biosciences, Faculty of Science, Universiti Teknologi Malaysia Johor Bahru, Malaysia

ABSTRACT

Twelve novel chalcones were synthesized using 2-alkyloxy-naphthaldehydes and Mannich bases of 4-hydroxyacetophenone. The chalcones were characterized using FTIR, 1D and 2D NMR and HRMS spectroscopy. Comparative docking analysis was carried out to screen their affinity towards the AChE enzyme (PDB 1EVE). All chalcones showed lower binding energy (-13.06 to -10.43 kcal/mol) against AChE better than donepezil (-10.52 kcal/mol). All chalcones were potent inhibitors towards AChE, with IC_{50} values ranging between 0.11 and 5.34 nM better than donepezil (IC_{50} 33.4 nM) and selectivity indexes (0.66–23.83), despite the fact that chalcones **10** and **13** were inactive. The structure activity relationship indicated that introducing diethyl amine in ring A of the chalcone skeleton and the propargyl moiety at ring B was affirmed to be a prospective drug against AChE. The multifunctional properties of chalcone **15** were all advantages that demonstrate an excellent candidate for the development of an effective drug against AChE.

1. Introduction

Cholinesterases (ChE), including Acetylcholinesterase (AChE) and Butyrylcholinesterase (BuChE), belong to serine hydrolase family; both enzymes are esterase catalyzing the hydrolytic breakdown of neurotransmitter acetylcholine (ACh) [1]. According to the classical cholinergic hypothesis, AChE terminates the neurotransmission at the cholinergic synapse by hydrolyzing the neurotransmitter ACh causing the cognitive impairment in Alzheimer's disease (AD) patients [2,3]. AChE and BuChE differ in kinetics and substrate selectivity since the BuChE lacks six aromatic amino acids out of the fourteen that line the catalytic gorge of AChE [4,5]. Strong evidence of the correlation between high selectivity for AChE versus BuChE and therapeutic index of the inhibitor was investigated *in vivo* by Liston *et al.* [6]. It was suggested that high selectivity for AChE might contribute to the clinically favourable tolerability profile of drugs in Alzheimer's disease patients. AChE inhibitors are still the best available pharmacotherapy for AD patients [7].

The Food and Drug Administration approved (FDA) treatments for AD belong to a category of acetylcholinesterase inhibitors (AChEIs) namely rivastigmine, donepezil, and galantamine [8–10]. Although Tacrine was the first drug approved for the AD treatment in 1993, it was withdrawn from the market because of a high incidence of hepatotoxicity [11]. Unfortunately, most of the commercial medications were observed to be associated with adverse side effects [12]. Hence, the search for novel AChE is still of great interest.

Recently, it became a trend to use natural products such as chalcones in discovering cholinesterase inhibitors due to their slight side-effects [13]. Chalcone based derivatives have gained attention due to their simple structures with diverse pharmacological actions [14]. The presence of a reactive α, β-unsaturated keto function in chalcones, is found to be responsible for their bioactivities. In the past years, a variety of chalcones have been reviewed to highlight the recent evidence of chalcone as a privileged scaffold in medicinal chemistry [15–17]. Fascinatingly, it has been reported that some chalcone derivatives can be considered as a multifunctional agent for AD treatment [18]. By screening AChEIs inhibitors in clinical application, some researchers claimed that amino substituent was possibly important pharmacophore of them [19]. Thereby, a series chalcone derivates containing amino substituents were designed and synthesized in their investigations [20,21]. Their results suggested that dimethylamine, diethylamine, dipropylamine, pyrrolidine-containing chalcones had more

Figure 1. Flavokawin B.
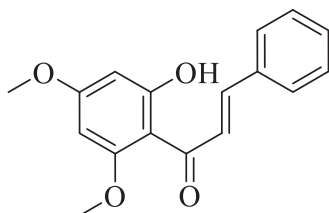

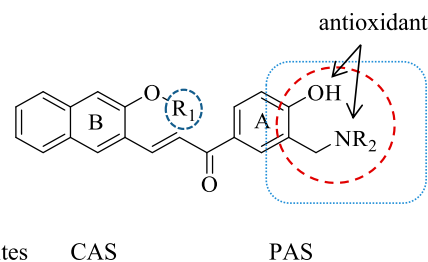**Figure 2.** Designed of aminoalkylated naphthalene-based chalcones.

potent effects in inhibiting AChE compared with other nitrogen-containing chalcones.

Liu *et al.* (2014) were inspired to synthesize novel cholinesterase inhibitors by introducing Mannich bases to the well-known chalcone flavokawin B due to its diverse bioactivities (Figure 1). As a matter of fact, the AChE inhibitory activity was poor for the parent compound (IC$_{50}$ > 500 μM). However, most of its Mannich base derivatives were potential AChE inhibitors especially piperidine derivative, which was more active than rivastigmine by two-fold. Meanwhile, it can bind with both the catalytic site and the peripheral site of AChE binding pocket according to the molecular docking result[22].

Furthermore, many researchers have argued that molecules bearing phenolic Mannich base moieties may exhibit good antioxidant, AChE inhibitory activity and chelating metal properties [23–25]. It has conclusively been shown that targets with these properties have been majorly included in the multi-target directed ligands regimen (MTDLs) of AChE inhibitors [2]. More recent studies in AD have confirmed that incorporate Mannich bases moiety and chalcone scaffold in one pharmacophore exerted moderate inhibitory potency for EeAChE with good multifunctional properties [26,27].

This project emphasizes on structure-based drug design of AChE inhibitors following the MTDLs approach to design chalcone analogues. Assuming that the novel synthesized chalcones will be an efficient AChE inhibitor with antioxidant property.

Recent evidence suggests that the presence of a different ring or fused ring system, make the drug structure more rigid [28]. This rigidity improves the probability of binding to the active site in the correct conformation. Hence, we aimed to introduce naphthalene in a chalcone skeleton to satisfy the primary structural necessity for the deep hydrophobic active site, as presented in Figure 2. Moreover, we proposed side chain R$_1$ to form three different alkoxy derivatives, namely propyloxy, propargyloxy and benzyloxy. This modification was done to increase the probability of cation-π interaction between the proposed ligands and the CAS residues. Likewise, the discrepancy of the side alkyl chain on the naphthalene motif was to facilitate the interaction with the high aromatic content of gorge walls.

Additionally, recent evidence suggests that a tertiary amino group on the alkyl side chain is the critical requirement for the potent AChE inhibition in the chalcone backbone [22,29]. Thus, modifications of the chalcone primary scaffold's by incorporating Mannich base moiety is crucial. These chemical variations on NR$_2$ were considered to form a metal-chelation and antioxidant sites that might target the PAS residues. Thereby, a series of chalcone derivatives containing amino substituents NR$_2$ were designed and synthesized in this work. According to figure 2, possible chemical modifications will take place through R$_1$ and NR$_2$R$_3$ using three different alkyl groups (R$_1$: propyl, propargyl and benzyl groups) and four various secondary amines (NR$_2$R$_3$: piperidine, morpholine, pyrrolidine and diethylamine). Moreover, *in silico* investigations are used to simulate the compounds binding interactions with the target to highlight their affinity before embarking on the *in vitro* assessment. Furthermore, it is an essential tool combined with the practical results to determine the SAR of the novel chalcones as AChEIs.

2. Results and discussion

2.1. Synthesis of chalcone derivatives

The known precursors **2(a-c)** were obtained via SN2 nucleophilic substitution reaction of commercially available 2-hydroxynaphthaldehyde **(1)** with alkyl halide under basic conditions using the sonication procedure in good to excellent yields as reported in the literature [30–32]. Simultaneously, Mannich bases **4 (a-d)** were prepared in a one-step condensation reaction of 4-hydroxyacetophenone **(3)**, formaldehyde and different secondary amines using microwave irradiations according to our published method [33].

The target chalcones were obtained via Claisen–Schmidt condensation reaction of 2-alkoxy naphthaldehyde derivatives **2(a-c)** with appropriate Mannich bases of 4-hydroxyacetophenone **4 (a-d)** using a catalytic amount of SOCl$_2$ in ethanol to furnish the novel chalcones **5–16** in an excellent yield (83-98%) as illustrated in Scheme 1. The structures of the newly chalcones **5–16** were characterized based on their spectroscopic analysis. Chalcone **6** was chosen as a model to verify the pattern of such compounds (Figure 3). The IR spectrum
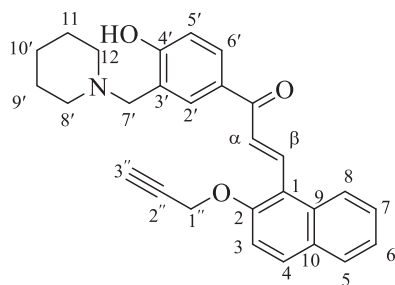
Figure 3. Chalcone 6.

Table 1. NMR Spectroscopic Data of chalcone **6.**

Position	δ_H	δ_C	COSY	HMBC
1	-	132.59		
2	-	155.29		
3	8.06 (d, $J = 9.2$ Hz)	132.44	H-4	C-2, C-1
4	7.59 (d, $J = 9.2$ Hz)	115.25	H-3	C-2, C-3, C-9
5	8.20 (d, $J = 8.8$ Hz)	123.61	H-6	C-7, C-9, C-10
6	7.61 (t, $J = 7.3$ Hz)	128.35	H-5, H-7	C-10
7	7.46 (t, $J = 7.3$ Hz)	124.77	H-6, H-8	C-5, C-9
8	7.95 (d, $J = 7.6$ Hz)	127.63	H-7	C-1, C-6, C-10
9	-	129.49		
10	-	117.95		
α	7.97 (d, $J = 16.0$ Hz)	129.22	H-β	C = O, C-1
β	8.27 (d, $J = 16.0$ Hz)	136.26	H-α	C-1, C-2, C = O, C-α
1'	-	129.72		
2'	8.29 (d, $J = 2.0$ Hz)	135.31	H-6'	C-4', C-7'
3'	-	116.90		
4'	-	161.94		
5'	7.17 (d, $J = 8.5$ Hz)	116.37	H-6'	C-3', C-1', C4'
6'	8.07 (dd, $J = 8.5, 2.0$)	132.10	H-5', H-2'	C-α, C-4', C-2'
7'	4.26 (s)	53.85		C-8', C-2', C-3', C4'
8'	2.92 (br s)	52.25		
9', 11	1.75 (br s)	22.73		
10'	1.38 (br s)	21.66		
12	3.31 (br s)	52.25		
''1	5.15 (d, $J = 2.4$ Hz)	57.27	H-3''	C-2, C-2'', C-3''
''2	-	79.77		
''3	3.68 (t, $J = 2.2$ Hz)	79.18	H-1''	C-2''
C = O	-	187.98		

Experimental data measured at 400 MHz in DMSO

of compound **6** showed a broad absorption band at 3433 cm^{-1} for hydroxyl group and stretching vibration at 2938 cm^{-1} for aliphatic CH (sp^3). Also, it displayed absorption frequency at 1645 cm^{-1} indicating the presence of conjugated carbonyl group besides the characteristic band C=C, olefinic peak at 1602 cm^{-1} and absorption band of C-N at 1297cm^{-1}. Furthermore, it revealed the presence of sharp, weak absorptions at 2122 and 3242 cm^{-1} represented the typical characteristic of C≡C and C-H sp stretching of the terminal alkyne, respectively.

Moreover, ^{1}H NMR spectrum confirmed the formation of chalcone **6** due to the presence of an AB spin system at δ_H 7.97 and 8.27 ($J = 16.0$ Hz each) attributed to H-α and H-β. These two doublets are characteristic of *trans*-olefinic protons of chalcone. The spectrum also disclosed an ABX spin system at δ_H 8.29 (1H, d, $J = 2.0$ Hz, H-2'), 8.07 (1H, dd, $J = 8.5$ and 2.0 Hz, H-6') and 7.17 (1H, d, $J = 8.5$ Hz, H-5') attributed to three aromatic protons in the A ring. While the prominent triplet signal at δ_H 3.68 and doublet peak at the downfield region δ_H 5.15 were attributed to propargyl protons'

H-3'' and H-1'', respectively. Interestingly, this multiplicity pattern is due to long-range ^{1}H−^{1}H couplings between H-3'' and H-1'' as depicted in the COSY spectrum (Supplementary Figure S5). Additionally, DEPT and ^{13}C NMR spectra of chalcone **6** displayed three signals at downfield region δ_C 57.27 (C-1'', CH$_2$), 79.77 (C-2'', C), 79.18 (C-3'', CH) which confirmed the existence of propargyl moiety. The HMBC spectrum of chalcone **6** supported the assignment of the quaternary carbons and the connectivity within the carbon framework. For example, a long range ^{1}H−^{13}C correlations were observed between H-α (δ_H 7.97) and H-β (δ_H 8.27) with C-1(δ_C 132.59) and carbonyl carbon (δ_C 187.98), H-β (δ_H 8.27) with C-α (δ_C 129.22) and C-2 (δ_C 155.29). The protons and carbons assignment of chalcone **6** was also supported and reconfirmed by HMQC and HMBC spectra. The pseudo molecular ion peak detected at *m/z* 426.2064 [M + H]$^+$ (calcd. 425.1991) recorded in the HRESIMS spectrum was in good agreement with the molecular formula C$_{28}$H$_{27}$NO$_3$. The complete elucidation of chalcone **6** is listed in Table 1.

2.2. *In silico forecasts drug properties prediction of library compound/chalcone derivatives*

Although considerable efforts were devoted to achieve selectivity for AChE as a target, and indeed, these days, many ligands endowed with outstanding *in vitro* selectivity are available [34]. However, it should be noted that a highly selective ligand for a given target does not always result in a clinically efficient drug. Experimental *in vivo* investigations of such drugs are not only significantly intricate but also expensive. Computational methods such as docking are commonly used to simulate the ligand interactions with the target to highlight its affinity. Apart from the docking functions, computational biology approaches have led the researchers to have an idea of structure–activity relationship (SAR) and pharmacokinetic properties (absorption, distribution, metabolism, excretion, and toxicity or ADMET) of the potential ligands [35]. The application of various computational tools, thus, helps save time that was spent in traditional combinatorial chemistry screening experiments [36].

2.2.1. *In silico prediction of physiochemical properties, drug likeness and bioactivity of the synthesized chalcones*
The analyses of the physiochemical properties have been widely used to filter out compounds with undesirable properties, especially poor ADMET profile [37]. Furthermore, drug-likeness is another characteristic, which provides the base for the compound to be an efficient drug candidate. The most famous drug-likeness filter the "Rule of Five" has been proposed by Lipinski *et al.*[38], which provides five rules to determine whether a molecule is well orally absorbed or

Table 2. Physicochemical properties and drug-likeness of synthesized chalcones **5-16.**

Compound No.	Physicochemical properties						Drug Likeness		
	Mol. Wt.	RB	HBA	HBD	TPSA	ilogP	Lipinski	Bioavailability Score	Drug Likeness Score
5	429.55	8	4	1	49.77	4.41	Yes	0.55	1.88
6	425.52	7	4	1	49.77	3.93	Yes	0.55	1.61
7	477.59	8	4	1	49.77	4.06	Yes	0.55	1.45
8	415.52	8	4	1	49.77	4.37	Yes	0.55	1.78
9	411.49	7	4	1	49.77	3.63	Yes	0.55	1.51
10	463.57	8	4	1	49.77	3.85	Yes	0.55	1.36
11	431.52	8	5	1	59.00	3.96	Yes	0.55	1.68
12	427.49	7	5	1	59.00	4.09	Yes	0.55	1.41
13	479.57	8	5	1	59.00	4.17	Yes	0.55	1.28
14	4.17.54	10	4	1	49.77	4.29	Yes	0.55	1.36
15	413.51	9	4	1	49.77	3.87	Yes	0.55	1.20
16	465.58	10	4	1	49.77	4.24	Yes	0.55	1.08

RB, number of rotatable bonds; HBD, number of hydrogen bond donor and acceptor (HBA); TPSA, total polar surface area.

not: molecular weight (MW) $\leq$ 500, octanol/water partition coefficient (ClogP) $\leq$ 5, number of hydrogen bond donors (HBD) $\leq$ 5 and number of hydrogen bond acceptors (HBA) $\leq$ 10. If a compound violates two or more rules, it may not be orally active. Topological Polar Surface Area (TPSA) is a parameter used to analyze drug transport across a membrane such as for gastrointestinal absorption, Caco-2 monolayer permeability and blood–brain barrier penetration, which correlates with its bioavailability score [39]. SwissADME Web tool was used to assess the drug-likeness properties of chalcone compounds. All chalcones are found to follow the Lipinski Rule of five without any violation, as shown in Table 2. Compounds with TPSA values less than 140 demonstrated high oral bioavailability or cell permeability. All chalcones' TPSA calculations were within the required limit (49.77 or 59 Å) and the bioavailability score [40]. The novel chalcones are most likely to be a drug, as their drug-likeness scores range from 1.08-1.88.

The Molinspiration server was used to predict the bioactivity of the synthesized chalcones. The bioactivity scores in Table 3 indicate that all chalcones are likely to be active drugs towards GPCR ligands, nuclear receptor ligands and other enzyme targets. Besides, chalcone derivatives are moderately active towards kinase inhibitors, ion channel modulators and protease inhibitors. Though, for more specific target prediction, the Swiss Target Prediction server was used [41]. Strikingly, the target prediction result confirms our suggestions that the modified chalcones could be an AChE inhibitor, as exemplified in Figure 4.

2.2.2. In silico pharmacokinetic and toxicity predictions of chalcones 5–16

Pharmacokinetic and toxicity screening are tabulated in Tables 4 and 5. All tested derivatives **5–16** have shown high gastrointestinal (GI) absorption, which is a good indicator of oral bioavailability. Also, most of the chalcones have shown blood–brain permeability except compounds **7**, **10**, **14**, **16**. The ability to cross the BBB is an essential feature for the potency of AChE inhibitors. All chalcones are P-gp inhibitors, implies that active

Table 3. Molinspiration bioactivity score.

Compd. No.	GPCR	ICM	KI	NRL	PI	EN
5	0.07	−0.11	−0.18	0.04	−0.07	0.05
6	0.13	−0.16	−0.16	0.08	−0.03	0.09
7	0.09	−0.09	−0.12	0.03	0.00	0.08
8	0.07	−0.11	−0.17	0.05	−0.02	0.05
9	0.13	−0.15	−0.14	0.09	0.02	0.09
10	0.09	−0.06	−0.11	0.04	0.04	0.08
11	0.01	−0.18	−0.16	0.01	−0.09	0.02
12	0.07	−0.23	−0.13	0.05	−0.06	0.06
13	0.03	−0.15	−0.10	0.01	−0.03	0.04
14	0.04	−0.15	−0.2	0.01	−0.12	0.03
15	0.09	−0.21	−0.18	0.06	−0.09	0.06
16	0.05	−0.11	−0.14	0.01	−0.06	0.05

GPC, GPCR ligand; ICM, ion channel modulator; KI, kinase inhibitor; NRL, nuclear receptor ligand; PI, protease inhibitor; EI, enzyme inhibitor; active drug (score > 0); moderately active drug (0 > score > −5); inactive drug (score < −5).

Table 4. Pharmacokinetic predictions using SwissADME.

Compound No.	GI absorption	BBB permeant	P-gp	CYP2C19 inhibitor	CYP2D6 inhibitor
5	High	Yes	Yes	Yes	Yes
6	High	Yes	Yes	Yes	Yes
7	High	No	Yes	No	Yes
8	High	Yes	Yes	Yes	Yes
9	High	Yes	Yes	Yes	Yes
10	High	No	Yes	Yes	Yes
11	High	Yes	Yes	Yes	Yes
12	High	Yes	Yes	Yes	Yes
13	High	Yes	Yes	Yes	No
14	High	No	Yes	Yes	Yes
15	High	Yes	Yes	Yes	Yes
16	High	No	Yes	Yes	Yes

GI, gastrointestinal; P-gp, P-glycoprotein; BBB, blood–brain barrier; CYP2C19 and CYP2D6, cytochrome P450.

efflux across biological membranes is not possible. All chalcones were inhibitors for CYP2C19 and CYP2D6 implicating potential increased in other drug concentration as these compounds might not be metabolized by the liver enzymes hence accumulate inside the body except chalcones except **7** and **13**. Toxicity screening showed that all chalcones are noncarcinogenic and non-mutagenic, excluding compound **16**, which is predicted to be mutagenic. The computed LD_{50} in the rat from the acute toxicity prediction appears to be adequately benign in the range between 2.56 and 2.82 mol/kg.
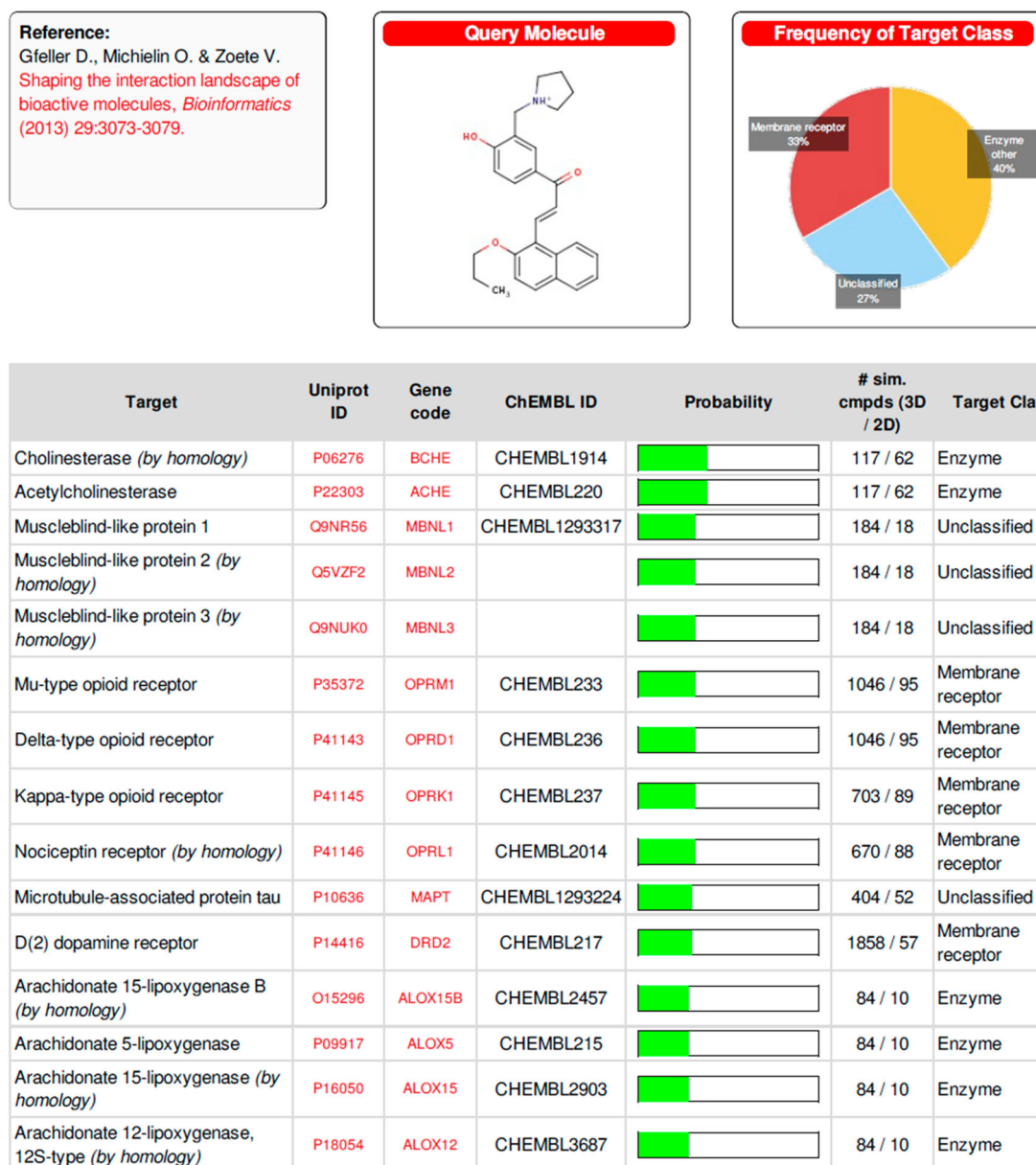
SwissTargetPrediction report:

Reference:
Gfeller D., Michielin O. & Zoete V. Shaping the interaction landscape of bioactive molecules, *Bioinformatics* (2013) 29:3073-3079.

Query Molecule

Frequency of Target Class

Target	Uniprot ID	Gene code	ChEMBL ID	Probability	# sim. cmpds (3D / 2D)	Target Class
Cholinesterase *(by homology)*	P06276	BCHE	CHEMBL1914		117 / 62	Enzyme
Acetylcholinesterase	P22303	ACHE	CHEMBL220		117 / 62	Enzyme
Muscleblind-like protein 1	Q9NR56	MBNL1	CHEMBL1293317		184 / 18	Unclassified
Muscleblind-like protein 2 *(by homology)*	Q5VZF2	MBNL2			184 / 18	Unclassified
Muscleblind-like protein 3 *(by homology)*	Q9NUK0	MBNL3			184 / 18	Unclassified
Mu-type opioid receptor	P35372	OPRM1	CHEMBL233		1046 / 95	Membrane receptor
Delta-type opioid receptor	P41143	OPRD1	CHEMBL236		1046 / 95	Membrane receptor
Kappa-type opioid receptor	P41145	OPRK1	CHEMBL237		703 / 89	Membrane receptor
Nociceptin receptor *(by homology)*	P41146	OPRL1	CHEMBL2014		670 / 88	Membrane receptor
Microtubule-associated protein tau	P10636	MAPT	CHEMBL1293224		404 / 52	Unclassified
D(2) dopamine receptor	P14416	DRD2	CHEMBL217		1858 / 57	Membrane receptor
Arachidonate 15-lipoxygenase B *(by homology)*	O15296	ALOX15B	CHEMBL2457		84 / 10	Enzyme
Arachidonate 5-lipoxygenase	P09917	ALOX5	CHEMBL215		84 / 10	Enzyme
Arachidonate 15-lipoxygenase *(by homology)*	P16050	ALOX15	CHEMBL2903		84 / 10	Enzyme
Arachidonate 12-lipoxygenase, 12S-type *(by homology)*	P18054	ALOX12	CHEMBL3687		84 / 10	Enzyme

Figure 4. An example of the Swiss Target Prediction report of chalcone **8**.
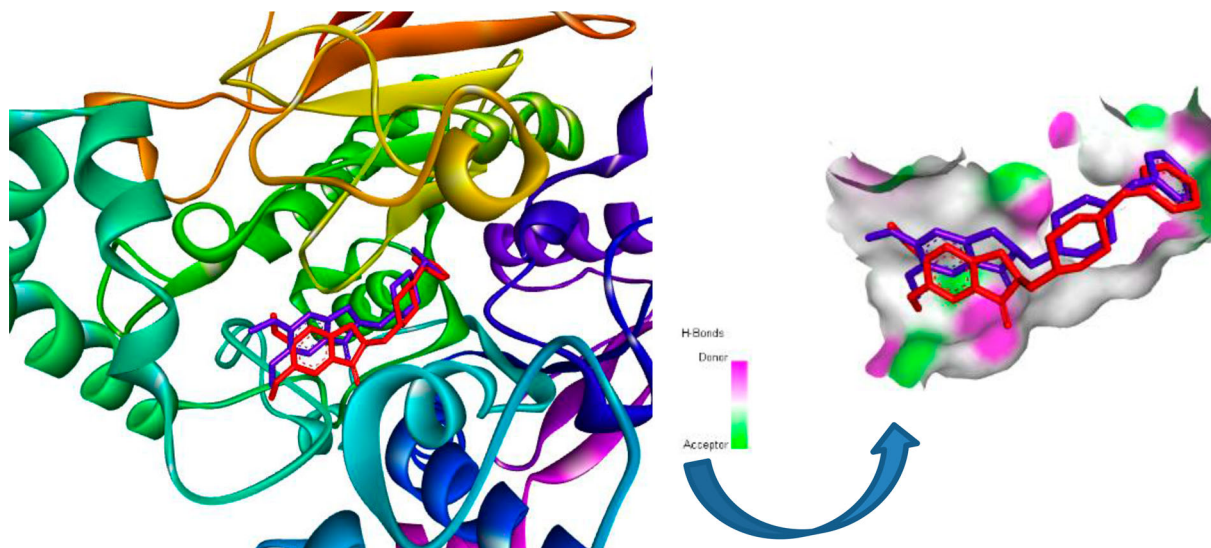
2.2.3. Molecular docking

Comparative docking analysis was carried out on twelve different chalcone derivatives to screen their binding affinity on the *Torpedo california* acetylcholinesterase (TcAChE) (PDB 1EVE). Firstly, to validate the docking parameter, the co-crystalized ligand donepezil (E20) was re-docked into the active site of the AChE enzyme. The parameters are considered successful with Root Mean Square Deviation (RMSD) value of the docking structure is less than 1.5 Å and the ligand orientation display similar interactions as reported in the crystal structure [42]. The validation experiment is illustrated in Figure 5, which shows the superimposition of both the re-docked donepezil (red) and its respective conformation in the crystal structure (blue) within the active site

of AChE, indicating that the selected docking parameters are acceptable. The RMSD value for docking conformation is 1 Å. Docking analysis of the synthesized chalcone derivatives **5–16** demonstrated lower binding energy than donepezil (−10.52 kcal/mol) indicating increased in affinity towards AChE enzyme as illustrated in Figure 6.

The interaction mode of the docked chalcones demonstrated that the piperidine moiety in chalcones **5** and **7,** was stacked against the amino acids PHE331 and TRP84 at the anionic site, respectively, whereas, in chalcone **6**, it was stacked against TYR334in PAS (see Appendix, Tables S41-S44). Moreover, it illustrated that diethyl amine moiety in chalcone **14** possessed a flexible structure that enabled it to be stacked against

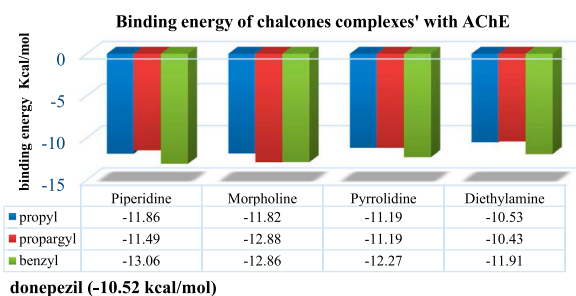**Table 5.** Toxicity predictions of the synthesized chalcones using admetSAR.

Compound Number	Mutagenicity Ames Test	Carcinogenicity	Acute Oral Toxicity mol/kg
5	🟩	🟩	2.60
6	🟩	🟩	2.82
7	🟩	🟩	2.81
8	🟩	🟩	2.61
9	🟩	🟩	2.78
10	🟩	🟥	2.77
11	🟩	🟩	2.69
12	🟩	🟩	2.82
13	🟩	🟩	2.82
14	🟩	🟩	2.56
15	🟩	🟩	2.80
16	🟥	🟩	2.77

Figure 5. Superimposition of docking conformation of TcAChE-donepezil complex (red stick) and its crystal structure (blue stick) (PDB: 1EVE).

Table 6. DPPH radical scavenging activity of the chalcones **5-16.**

Compound	DPPH Radical IC$_{50}$ µg/ml
5	39.68 ± 0.9
6	42.47 ± 1.8
7	55.52 ± 1.1
8	41.66 ± 1.5
9	12.57 ± 0.8
10	19.34 ± 0.7
11	42.10 ± 1.3
12	35.36 ± 1.5
13	42.70 ± 1.1
14	44.50 ± 0.7
15	40.58 ± 1.7
16	37.52 ± 1.8
Ascorbic acid	17.96 ± 0.4

Figure 6. Lowest binding energy of the top-ranked conformations of the resulted complexes of docking experiments.

TRP279 while in chalcone **15** and **16**, the same moiety stacked against TRP84. Meanwhile, the pyrrolidine moiety in chalcone **8** stacked against PHE331 and TRP279 in chalcones **9** and **10**. Whereas the morpholine moiety in chalcones **11, 12** was stacked against the anionic site (PHE331), but in chalcone **13,** it showed interaction with the acyl pocket amino acid (PHE288).

To consider the overall efficacy for chalcones as AChEIs in terms of substitution at ring B, it was necessary to screen the binding profiles of chalcone derivatives in depth. As a comparison, it was found that chalcone **5** showed competitive inhibition via direct catalytic active sites (CAS) only among propyl series. In contrast, the remaining derivatives of the propyl series demonstrated several potent interactions with the CAS and weak interaction with PAS without any interaction with the critical amino acid TRP279, despite chalcone **14**. For the propargyl series, the binding network of **9** revealed non-competitive inhibition due to the absence of the interaction with the CAS residues, especially Trp84, as presented in Figure 7. At the same time, chalcone **15** exhibited CAS and PAS's dual binding site inhibitor. The overlay of the AChE-**15** complex with the complex of
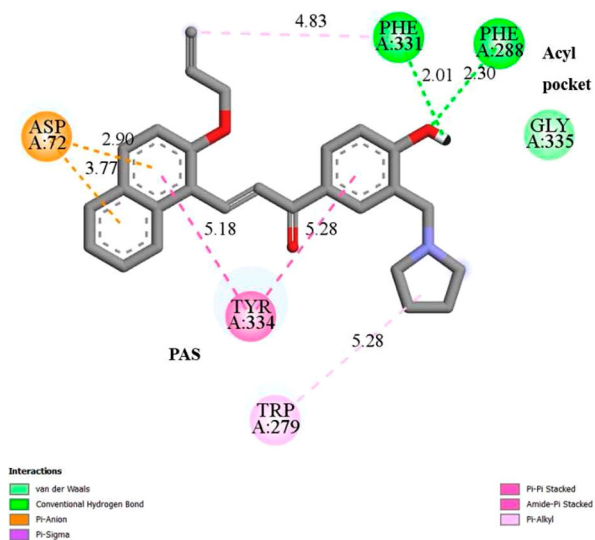
Figure 7. 2D representation of the interaction modes of chalcone **9.**

Figure 8. The overlay of the AChE-**15** complex (grey stick) with the complex of AChE-donepezil (grey stick and balls) at the active gorge.

AChE-donepezil at the active gorge showed the structural resemblance of **15** to donepezil, as postulated in Figure 8. The flexible diethyl amine moiety has a unique orientation at the CAS; thus, two hydrophobic interactions were observed between one ethyl group and the phenyl and indole ring of TRP84. The second ethyl group was connected to the phenyl ring of Phe331 with a hydrophobic interaction. Moreover, hydrophobic interactions were observed between the diethyl group in chalcone **15** and the imidazole ring of HIS440, the critical amino acid at the catalytic traid. On the other hand, it was found that the number of hydrogen bonds decreased in the benzyl series comparable with the propyl and propargyl series based on the binding profiles.

2.3. Bioactivities

2.3.1. DPPH radical scavenging activity

The radical scavenging potential of chalcone derivatives **5–16** with ascorbic acid (AA) as positive control is shown in Table 6. All chalcones displayed potent DPPH radical scavenging activity (IC$_{50}$ 12.57-55.52 µg/ml). It is interesting to note that chalcones **9** and **10** were the most potent antioxidant with IC$_{50}$ 12.57 and 19.34 µg/ml, respectively. All chalcones were found to scavenge DPPH in a dose-dependent manner, as portrayed in Figure 9. Chalcones **5–16** owning hydroxyl group at para position in ring A that readily reacted with the radicals and converted to phenoxy radical due to the electron delocalization of the relative coplanar structure of the chalcone, which also responsible for the excellent scavenging activity [43].

2.3.2. Cholinesterases enzyme inhibitory activity

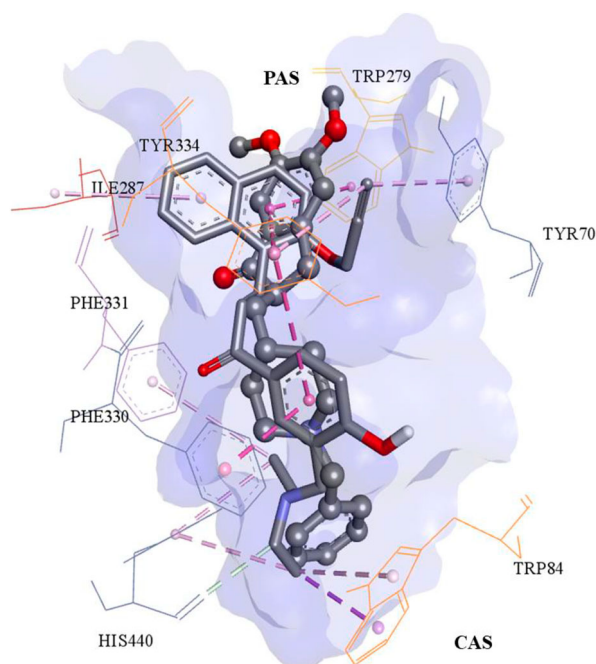Ellman's spectrophotometric method was followed as described by Koay et al. to evaluate the cholinesterase
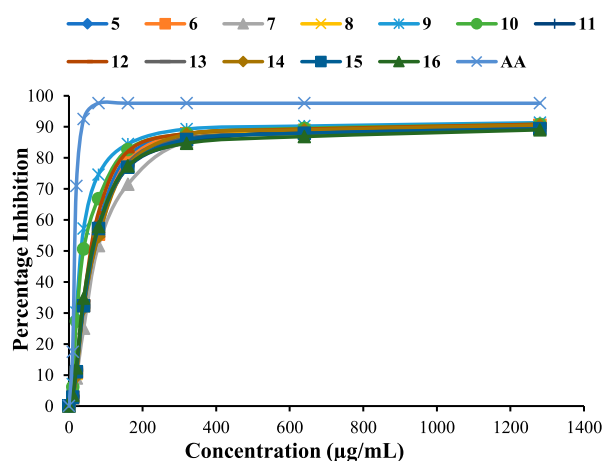
Figure 9. Percentage inhibition DPPH radical of the chalcones **5–16.**

inhibitory activities of chalcones **5–16** [44]. The AChE from an electric *eel*, BuChE from an equine serum and donepezil as the reference standard was utilized for this evaluation, as shown in Table 7, Figures 10 and 11. It is apparent from this table that chalcones **5–16** clearly showed higher potency against AChE (IC$_{50}$ ranging from 0.11–5.34 nM) than donepezil (IC$_{50}$ 33.4 nM) despite chalcones **10** and **13**. The present findings seem to be generally consistent with the docking results, which suggested that chalcones bearing the Mannich base might be better inhibitors than donepezil. Besides, all synthesized chalcones were found to be more effective inhibitors towards AChE than BuChE, with high selectivity indexes (0.66–23.83).
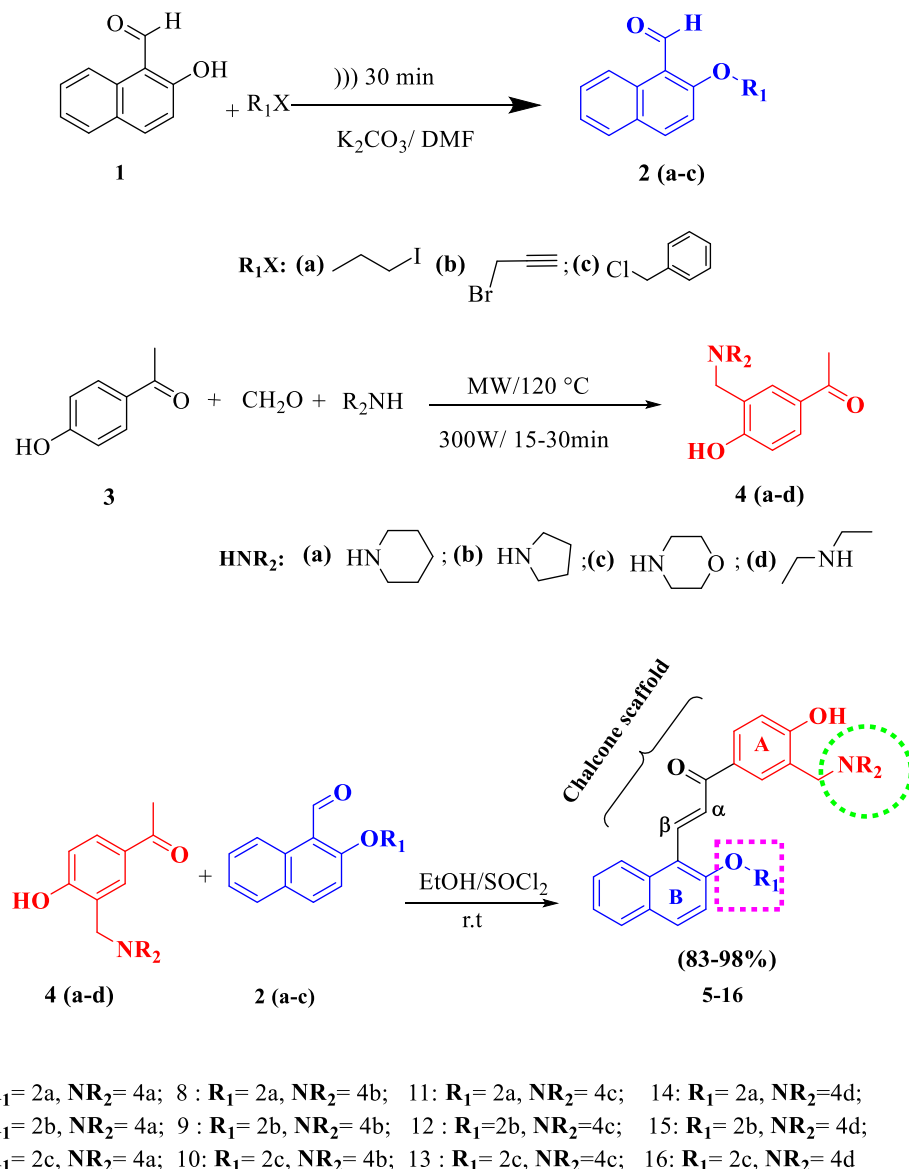
Scheme 1. Synthesis of 2-alkoxynaphthyl chalcone bearing Mannich bases 5–16.

5 : R_1= 2a, NR_2= 4a; 8 : R_1= 2a, NR_2= 4b; 11: R_1= 2a, NR_2= 4c; 14: R_1= 2a, NR_2=4d;
6 : R_1= 2b, NR_2= 4a; 9 : R_1= 2b, NR_2= 4b; 12 : R_1=2b, NR_2=4c; 15: R_1= 2b, NR_2= 4d;
7 : R_1= 2c, NR_2= 4a; 10: R_1= 2c, NR_2= 4b; 13 : R_1= 2c, NR_2=4c; 16: R_1= 2c, NR_2= 4d
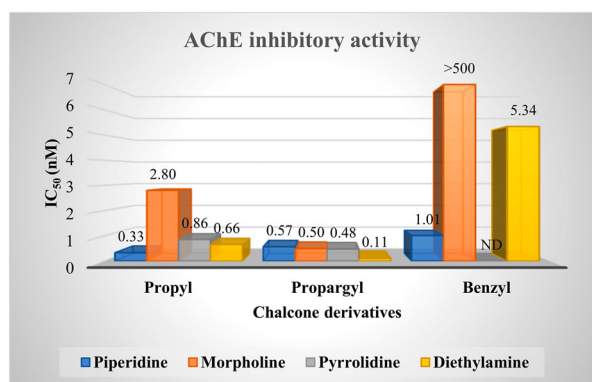
Figure 10. Effect of chalcones variation on AChE inhibitory activity.
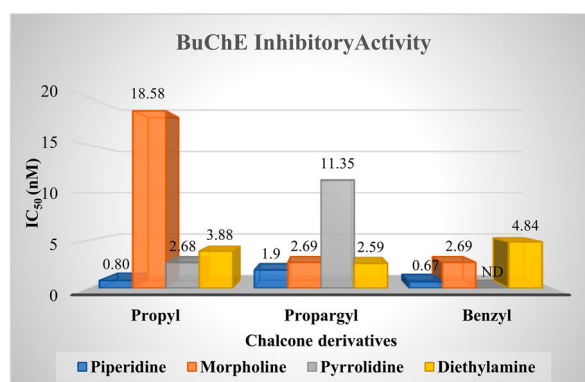
Figure 11. Effect of chalcones variation on BuChE inhibitory activity.

2.4. Structure–activity relationships

The *in vitro* studies declared that chalcone with a piperidine substituent is potent AChEIs excluding propargyl derivative. However, piperidine derivatives' potency was accompanied by lower selectivity indexes towards AChE ranging between 0.66–3.34. On the other hand, diethylamine derivatives disclosed higher efficacy and selectivity as AChEIs. While pyrrolidine derivatives **8–10**

Table 7. Cholinesterase inhibitory activity of chalcones 5-16.

| | IC$_{50}$ (nM) $\pm$ SD | | |
Compound	AChE	BuChE	SI
5	0.33 $\pm$ 0.002	0.80 $\pm$ 0.003	2.44
6	0.57 $\pm$ 0.005	1.90 $\pm$ 0.002	3.34
7	1.01 $\pm$ 0.003	0.67 $\pm$ 0.003	0.66
8	0.86 $\pm$ 0.004	2.68 $\pm$ 0.003	3.10
9	0.48 $\pm$ 0.003	11.35 $\pm$ 0.005	23.79
10	ND	ND	-
11	2.80 $\pm$ 0.001	18.58 $\pm$ 0.001	6.64
12	0.50 $\pm$ 0.015	2.69 $\pm$ 0.005	5.33
13	> 500	2.69 $\pm$ 0.003	-
14	0.66 $\pm$ 0.002	3.88 $\pm$ 0.005	5.89
15	0.11 $\pm$ 0.002	2.59 $\pm$ 0.003	23.83
16	5.34 $\pm$ 0.002	4.84 $\pm$ 0.002	0.91
Donepezil	33.4 $\pm$ 0.002	2246.0 $\pm$ 0.003	67.25

ND = not determined; IC$_{50}$ $\pm$ SD: Inhibitor concentration (mean $\pm$ SD of three experiments) needed for 50% inhibition of the enzyme; SI: selectivity index = IC$_{50}$(BuChE)/ IC$_{50}$(AChE).

were less potent than piperidine and diethylamine analogues with selectivity indexes (3.10 −23.79). It was evident that chalcones with a morpholine substituent at ring A demonstrated practically the lowest inhibitory activity towards AChE among the four series. These findings corroborate the ideas of Zhang *et al.* (2019). They suggested that the electron-withdrawing effects of oxygen atoms at the morpholine unit might reduce the electronic density of amines and further impact its protonation, affecting the interaction between the terminal nitrogen and AChE.

A correlation between the structure and inhibitory activity attributes of the novel chalcones towards AChE was established. In brief, modifications at ring A using different amines showed that introducing diethyl amine is favourable due to its flexibility that enabled the chalcone to be extended into the PAS and CAS region of the active site and increase AChE inhibition. This structural flexibility is absent when introduced cyclic amines such as piperidine, pyrrolidine or morpholine due to their structural rigidity. Moreover, introducing the hydrophilic cyclic amine morpholine demonstrated practically the lowest inhibitory activity towards AChE among the four series.

On the other hand, the general tendency for AChE inhibition from the perspective of substitution at ring B based on the *in vitro* analysis was propargyl > propyl > benzyl, as presented in the histogram illustration in Figure 6. However, this finding contrasts with pre-evaluations of docking simulations based on the binding affinity. The efficacy of the propargyl derivatives might be attributable to the high electron density and structural rigidity of the propargyl fragment when compared to propyl. Furthermore, it was predicted for propyl analogues that chalcone **11** (NR$_2$R$_3$: morpholine) had almost similar binding energy for chalcone **5** (NR$_2$R$_3$: piperidine) (Figure 4). Interestingly, the *in vitro* potency of **11** was eight folds lower than **5**. This distinctive difference in efficacy can be explained based on the binding profiles of both chalcones, as

presented in Appendix, Table S41, chalcone **5** showed three hydrogen bonds with critical amino acids of the active site SER200, HIS400 and PHE330, while chalcone **11** showed only one hydrogen bond with PHE330 at the anionic site with distance 2.13Å.

It is notable that propargylated chalcones **6, 9** and **12** (R$_2$: piperidine, pyrrolidine and morpholine) demonstrated nearly the same affinity against AChE, however, chalcone **9** was more selective to inhibit AChE with nearly four folds with SI = 23.79. This variation in the selectivity towards AChE was due to the missing interaction with TRP279 in chalcones **6** and **12**. It has been reported that TRP279 and PHE330 amino acid residues are conserved in AChE but absent in BuChE, which leads to the selectivity that may be important for clinical consideration, as inhibition of BuChE may cause potentiating side effects (Kryger *et al.*, 1999). Likewise, chalcone **15** (NR$_2$R$_3$: diethylamine) shows five folds higher potency than chalcone **6** (NR$_2$R$_3$: piperidine) with the highest selectivity index 23.83. Moreover, potency of chalcone **15** as AChEI increased by four folds from **9**, although both chalcones showed similar selectivity index towards AChE (SI = 23.79).

It is worth noting that increasing the aromaticity by introducing the benzyl moiety ended with a bulky structure of chalcone that selectively inhibits BuChE more than AChE, as presented in Figure 11. Moreover, the presence of the benzylic group causes a steric hindrance during the interaction between the chalcone and the amino acids residues of the receptor.

To sum it up, the modification at ring B using the propyl moiety led to a competitive inhibition via direct catalytic active site (CAS), which is unfavourable. Introducing the benzyl moiety at naphthalene ring ended with a bulky structure of chalcone that selectively inhibits BuChE more than AChE. Thus, it decreased the potential AChEI of the associated chalcones. The modification using propargyl disclosed characteristic dual interactions with amino acids of both the PAS and CAS of AChE binding site in a similar manner to the reference drug, donepezil.

3. Conclusion

Four series of aminoalkylated naphthalene-based chalcones **5–16** were synthesized successively through a Claisen–Schmidt condensation reaction. The condensation reaction was done using thionyl chloride between 2-alkoxynaphthaldehyde derivatives **2(a-c)** and Mannich bases **4(a-d)**. *In silico* predictions revealed that the novel chalcones are most likely to be a drug, as their drug-likeness scores range from 1.08-1.88. Pharmacokinetic screening disclosed that most of the chalcones were able to permeate through the BBB except chalcones **7,10,14** and **16**, while toxicity screening showed that all chalcones are noncarcinogenic and

non-mutagenic, excluding chalcone **16**, which is predicted to be mutagenic. The Swiss Target Prediction server was used to predict the suitable target for the synthesized chalcones. Consistently, the predictions confirmed our hypothesis regarding the selected target AChE before embarking the docking and the *in vitro* assessments.

Docking analysis was carried out on the acetylcholinesterase (*Tc*AChE) to compare the binding affinity of chalcone derivatives. The results predicted that all chalones **5–16** have a higher affinity compared with donepezil. Based on the bioactivities study, all of the chalcones were found to scavenge DPPH radicals with IC$_{50}$ values that ranged between 12.57 and 55.52 µg/ml. The cholinesterase inhibitory activities of the chalcones **5–16** were investigated *in vitro* using two enzymes AChE and BuChE, while the positive control was donepezil. Steadily with docking pre-evaluations, the novel chalcones **5–16** showed potent inhibitory activity against AChE (IC$_{50}$ 0.11-5.34 nM) more than donepezil (IC$_{50}$ 33.4 nM), despite that chalcones **10** and **13** were inactive against AChE. From the structural activity relationship (SAR), it is concluded that the potent dual site AChEI bears diethylamine at ring A and the propargyl moiety at ring B. Thus, among the promising candidates against AChE, chalcone **15** demonstrated enormous advantages, including an excellent AChE inhibitory activity, good antioxidant activity (IC$_{50}$ 40.58 µg/ml), low logP 3.87 and was able to permeate through the BBB. These multifunctional properties promoted **15** as an excellent candidate for the development of an effective drug against AChE.

4. Experimental

4.1. Chemistry

All solvents and reagents were purchased from Sigma-Aldrich and used without further purification. The monitoring of reaction was done by the utilization of pre-coated silica gel plates (60 F254), thin-layer chromatography (TLC). The normal phase silica gel (Merck, 70–230 mesh) was used to perform column chromatography (CC) purification, while the Merck silica gel (230-400 mesh) was utilized to perform the vacuum liquid chromatography (VLC). Melting points were measured using a Sanyo MPD350 apparatus with a digital display. A Perkin Elmer ATR spectrophotometer was used to record the infrared (IR) spectra without KBr. A Bruker Avance 400 MHz spectrometer was used to record ^{1}H NMR and ^{13}C NMR spectra. NMR samples were measured in DMSO, CDCl$_3$ and MeOD at room temperature. Mass spectral data were obtained from Mass Spectrometry Laboratory, King Abdulaziz University (Saudi Arabia). The absorbance data for bioactivity assays were recorded on BIOTEK Microplate reader (USA) spectrophotometer.

4.1.1. General synthesis of alkoxy naphthaldehydes (2 a-c)

2-Hydroxy-1-naphthaldehyde **(1)** (5.17 g, 30 mmol) was mixed with 36 mmol of potassium carbonate anhydrous in (60 mL) of N, N-dimethylformamide (DMF) as an aprotic solvent. This mixture was stirred at room temperature. Different alkyl halide, namely 1-Iodopropane, propargyl bromide, benzyl chloride (42 mmol), was added to the activated mixture and heated to 40 °C using ultrasound sonication for 30 min until the reaction complete. The mixture was cooled to room temperature and poured into crushed ice until precipitation. The resulting precipitate was filtered, washed with cold water, air-dried and recrystallized using ethanol. Three alkoxy-naphthaldehydes namely 2-propoxynaphthalene-1-carbaldehyde **(2a)**, 2-[(prop-2-yn-1-yl)oxy] naphthalene-1-carbaldehyde **(2b)** and 2-(benzyloxy) naphthalene-1-carbaldehyde **(2c)** were accomplished.

2-propoxynaphthalene-1-carbaldehyde (2a)

It was obtained as colourless crystals (4.5 g, 70%) with R$_f$ = 0.9 (*n*-hexane: EtOAc; 3:1), mp 63-65 °C (Lit. mp 63–64 °C [30]). IR:ν$_{max}$ cm^{-1} (ATR): 1663 (C = O), 2876 and 2805 (CHO), 2964 (C-H *sp^3*). ⊃1H NMR (400 MHz, CDCl3) 10.96 (1H, s, -CHO), 9.31 (1H, d, *J* = 8.8 Hz, H-8), 8.06 (1H, d, *J* = 9.2 Hz, H-3), 7.78 (1H, d, *J* = 8.0 Hz, H-5), 7.64 (1H, ddd, *J* = 8.4, 5.8, 1.2 Hz, H-6), 7.44 (1H, dd, *J* = 7.8, 0.8 Hz, H-7), 7.28 (1H, d, *J* = 9.2 Hz, H-4), 4.21 (2H, t, *J* = 6.4 Hz, OCH$_2$), 1.89-1.98 (2H, m, CH$_2$), 1.13 (3H, t, *J* = 7.4 Hz, CH$_3$).^{13}C NMR (100 MHz, CDCl3) δ 192.13 (C = O), 163.75 (C-2), 137.50 (CH), 131.59 (C), 129.79 (CH), 128.41 (C), 128.22, 124.92, 124.67 (CH), 116.72 (C), 113.58 (CH), 71.08 (OCH$_2$), 22.70 (CH$_2$), 10.58 (CH$_3$).

2-[(prop-2-yn-1-yl)oxy]naphthalene-1-carbaldehyde (2b)

It was obtained as colourless crystals (4.9 g, 77%) with R$_f$ = 0.8 (*n*-hexane: EtOAc; 3:1), mp 113-115 °C (Lit. mp 113–115 °C [31]). IR:ν$_{max}$ cm^{-1} (ATR): 1651 (C = O), 2117 (C≡C), 2893 and 2811 (CHO), 3250 (C-H *sp*). ⊃1H NMR (400 MHz, CDCl3): δ 10.92 (1H, s, CHO), 9.30 (1H, d, *J* = 8.8 Hz, H-8), 8.08 (1H, d, *J* = 9.0 Hz, H-3), 7.81 (1H, d, *J* = 8.0 Hz, H-5), 7.65 (1H, ddd, *J* = 8.4, 5.6, 1.2 Hz, H-6), 7.47 (1H, dd, *J* = 8.0, 0.8 Hz, H-7), 7.40 (1H, d, *J* = 9.0 Hz, H-4), 4.96 (2H, d, *J* = 2.4 Hz, OCH$_2$), 2.61 (1H, t, *J* = 2.4 Hz, ≡CH).^{13}C NMR (100 MHz, CDCl3): δ 192.00 (C = O), 161.90 (C-2), 137.31 (CH), 131.44 (C), 129.91 (CH), 129.11 (C), 128.26, 125.22, 125.11 (CH), 117.99 (C), 113.99 (CH), 77.68 (C≡C), 76.82 (≡CH), 57.38 (OCH$_2$).

2-(benzyloxy)naphthalene-1-carbaldehyde (2c)

It was obtained as colourless crystals (6.7 g, 85%) with R$_f$ = 0.9 (*n*-hexane: EtOAc; 3:1), mp 120-124 °C (Lit. mp 119 °C [32]). IR:ν$_{max}$ cm^{-1} (ATR): 3053 (C-H *sp^3*), 2884 and 2808 (CHO), 1659 (C = O).⊃1H NMR (400 MHz, CDCl3): δ 11.01 (1H, s, CHO), 9.31 (1H, d, *J* = 8.8 Hz, H-8), 8.06 (1H, d, *J* = 9.2 Hz, H-3), 7.79 (1H, d, *J* = 8.0 Hz, H-5), 7.65 (1H, dd, *J* = 8.2 Hz; 0.8 Hz, H-6), 7.35-7.49- (7H, m, H-4; H-7 and 5H of phenyl's group), 5.36 (2H, s, OCH$_2$).^{13}C NMR

(100 MHz, CDCl$_3$): δ 192.12(CHO), 163.21 (C-2), 137.54 (CH), 135.96, 131.57 (C), 129.93, 128.83 (CH), 128.70 (C), 128.44, 128.27 (CH),127.40, 125.01, 124.95 (CH), 117.20 (C), 113.95 (CH), 71.47 (OCH$_2$).

4.1.2. General synthesis of mannich base precursors (4 a-d)

To a solution of 4-Hydroxy-acetophenone (3) (16 mmol) and formaldehyde (CH$_2$O) (1.5 equivalent) in 1,4-dioxane (15 mL), was added to the corresponding secondary amine (piperidine (a), pyrrolidine (b), morpholine (c) or diethyl amine (d)) using the same equivalent of (3). This mixture was placed in the MW vessel with stirring and capped with a rubber cap. The reaction mixture was irradiated for 15-30 min, at 120°C (power 300 W)[33]. TLC was used to monitor the progress of the reaction. After the complete consumption of the starting materials, the vessel was removed and cool down to room temperature. The reaction mixture was concentrated under reduced pressure and purified using Column chromatography.

1-{4-hydroxy-3-[(piperidin-1-yl)methyl]phenyl}ethan-1-one (4a)

The reaction of compound (3), CH$_2$O and piperidine using the respective ratio 1:1.5:1.5 gave the crude product of (4a). The obtained product was purified using hexanes/ EtOAc (6:4) as an eluent over SiO$_2$ to yield (4a) as colourless crystals (2.15 gm, 58%) with R$_f$ = 0.55, mp 82-83°C. IR:v$_{max}$ cm^{-1} (ATR): 2946 (C-H sp^3),1661 (C = O),1594 (C = C),1284 (C-N),1259 (C-O). ^{1}H NMR (400 MHz, CDCl$_3$): δ 7.81 (1H, d, J = 8.4 and 2.2 Hz, H-6), 7.67 (1H, d, J = 2.2 Hz, H-2), 6.84 (1H, d, J = 8.4 Hz, H-5), 3.75 (2H, s, Benzylic-C**H$_2$**), 2.55 (7H, br s, 2×N-C**H$_2$**CH$_2$, CH$_3$),1.67 (6H, br s, 3×C**H$_2$**).^{13}C NMR (100 MHz, CDCl$_3$): δ 196.86 (C = O), 163.32 (C-4), 130.24 (C-6), 129.35 (C-2), 128.73 (C-1), 121.06 (C-3), 115.93 (C-5), 61.51 (Benzylic-**C**H$_2$), 53.73 (2×N-**C**H$_2$CH$_2$), 26.22 (CH$_3$), 25.60 (2×N-CH$_2$**C**H$_2$), 23.71 (N-CH$_2$CH$_2$**C**H$_2$). EIMS, *m/z* (% rel. intensity): 233 (10) [M$^+$, C$_{14}$H$_{19}$NO$_2$], 149 (4), 133 (2), 106 (1), 98 (5), 84 (100), 77 (3), 56 (2).

1-{4-hydroxy-3-[(pyrrolidin-1-yl)methyl]phenyl}ethan-1-one (4b)

A ratio of 1:1.5:1.5 of compound (3), CH$_2$O and pyrrolidine respectively were used to synthesize (4b). Eluting system of hexanes/ EtOAc (6:4), was used to purify the crude product to yield pale-yellow crystals, (1.72 g; 49%) with R$_f$ = 0.45, mp 92-95°C. IR:v$_{max}$ cm^{-1} (ATR): 2965 (C-H sp^3), 1661 (C = O), 1595 (C = C), 1287 (C-N), 1247 (C-O). ^{1}H NMR (400 MHz, MeOD): δ 7.83 (1H, dd, J = 8.6 and 2.2 Hz, H-6), 7.79 (1H, d, J = 2.2 Hz, H-2), 6.72 (1H, d, J = 8.6 Hz, H-5), 4.03 (2H, s, Benzylic), 2.92 (4H, t, J = 7.0 Hz, 2×NC**H$_2$**CH$_2$), 2.51 (3H, s, CH$_3$), 1.95-1.99 (4H, m, 2×NCH$_2$C**H$_2$**). ^{13}C NMR (100 MHz, MeOD): δ 197.75 (C = O), 167.15 (C-4), 130.73 (C-6), 130.22 (C-2), 126.14 (C-1), 121.21 (C-3), 116.53 (C-5), 57.13 (Benzylic-CH$_2$), 52.88 (2×N**C**H$_2$CH$_2$), 24.67 (CH$_3$), 23.02 (2×NCH$_2$**C**H$_2$). EIMS, *m/z* (% rel. intensity): 219(13)

[M$^+$, C$_{13}$H$_{17}$NO$_2$], 149 (5), 133 (3), 106, 91 (2), 84 (9), 77 (4), 70 (100), 51 (2).

1-{4-hydroxy-3-[(morpholin-4-yl)methyl]phenyl}ethan-1-one (4c)

The purification of the crude product which has been synthesized in the respective ratio of 1:1.5:1.5 of compounds (3), CH$_2$O and morpholine was done using column chromatography with hexanes/ EtOAc (8:2) as eluent to yield (4c) as colourless crystals (3.02 g; 80%) with Rf = 0.65, mp 69-70°C. IR:v$_{max}$ cm^{-1} (ATR): 2958 (C-H sp^3),1669 (C = O), 1597 (C = C), 1304 (C-N), 1113 (C-O). ^{1}H NMR (400 MHz, MeOD): δ 7.92 (1H, s, OH),7.83 (2H, s, H-2 and H-6), 3.73 (12H, t, J = 4.6 Hz, 2×Benzylic-CH$_2$ 4×OCH$_2$), 2.58 (8H, t, J = 4.0 Hz, 4×N-C**H$_2$**CH$_2$), 2.55 (3H, s, CH$_3$).^{13}C NMR (100 MHz, MeOD): δ 197.94 (C = O), 161.44 (C-4), 130.24 (C-2, C-6), 128.25 (C-1), 121.97 (C-3, C-5), 66.32 (4×OCH$_2$), 58.18 (2×Benzylic-CH$_2$), 52.78 (4×N-C**H$_2$**CH$_2$), 24.90 (CH$_3$). EIMS, *m/z* (% rel. intensity): 334(14) [M$^+$, C$_{18}$H$_{26}$N$_2$O$_4$], 276 (6), 247 (100), 217 (12), 189 (14), 162 (8), 133 (34), 119 (11), 86 (24), 56 (14).

1-{3-[(diethylamino)methyl]-4-hydroxyphenyl}ethan-1-one (4d)

The crude product of (4d) was obtained from the reaction of the respective ratio 1:2.1:2.1 of compound (3), CH$_2$O and diethyl amine. The product was purified by column chromatography using a mixture hexanes/ EtOAc (6:4) to yield (4d) as a yellow oily liquid (3.56 g, 99%) with R$_f$ = 0.56. IR spectrum (v_{max}/ cm^{-1}): 2972 (C-H sp^3), 1667 (C = O), 1589 (C = C), 1279 (C-N), 1255 (C-O). ^{1}H NMR (400 MHz, CDCl$_3$): δ 11.47 (1H, br s, OH), 7.73 (1H, d, J = 8.4 Hz, H-6), 7.60 (1H, s, H-2),6.74 (1H, d, J = 8.4 Hz, H-5), 3.77 (2H, s, Benzylic-C**H$_2$**), 2.59 (4H, q, J = 7.0 Hz, 2×NC**H$_2$**), 2.46 (3H, s, **CH$_3$**), 1.07 (6H, t, J = 7.0 Hz, 2×NCH$_2$C**H$_3$**). ^{13}C NMR (100 MHz, CDCl$_3$): δ 196.74 (C = O), 163.77 (C-4), 130.06 (C-6), 128.95 (C-2), 128.51 (C-1), 121.68 (C-3), 115.87 (C-5), 56.61 (Benzylic-**C**H$_2$), 46.22 (2×N**C**H$_2$CH$_3$), 26.08 (CH$_3$), 10.99 (2×NCH$_2$**C**H$_3$). EIMS, *m/z* (% rel. intensity): 221 (5) [M$^+$, C$_{13}$H$_{19}$NO$_2$], 206 (6), 149 (8), 132 (2), 106 (1), 77 (2), 58 (100).

4.1.3. General synthesis of naphthyloxy chalcones bearing Mannich bases

The corresponding precursors 4(a-d) and 2(a-c) were synthesized from 4-hydroxyacetophenone and 2-hydroxy-1-napthaldehyde, as described in the reported literatures [34,36,45]. A mixture of Mannich bases 4 (a-d) (1 mmol) and 2-alkoxy-1-naphthaldehyde 2 (a-c) (1 mmol) in 10 mL of ethanol was stirred at room temperature. A catalytic amount of thionyl chloride SOCl$_2$ was added dropwise, and the reaction mixture was kept overnight at room temperature. The reaction was monitored by TLC. After the reaction completion, the crude was allowed to stand under the cold condition for 2 h. The mixture was filtered or evaporated under reduced pressure to give the precipitate.

The resulting solid was subjected to column chromatography on silica gel using a mixture of $CHCl_3$ and EtOH (9.9:0.1) as an eluent to yield the pure target chalcone.

E-1-[3-(piperidin-1-yl)methyl-4-hydroxyphenyl]-3-(2-propoxynaphthal-en-1-yl) -2-propen-1-one (5)

Compound **4a** (0.23 g, 1 mmol) and **2a** (0.21 g, 1 mmol) was treated as described above. The desired chalcone **5** was obtained as yellow powder (0.42 g, 98%) with R_f = 0.35 (EtOH: $CHCl_3$; 1:9), mp 200-202°C. IR: v_{max} cm^{-1} (KBr): 3434 (OH), 2952 (C-H sp^3), 1638 (C = O), 1604 (C = C) and 1291 (C-N). ^{1}HNMR (400 MHz, DMSO): δ 8.24 (1H, d, J = 15.4 Hz, H-β), 8.15 (1H, d, J = 2.0 Hz, H-2'), 8.09 (1H, d, J = 8.8 Hz, H-5), 7.94 (1H, d, J = 9.0 Hz, H-3), 7.94 (1H, dd, J = 8.6 and 2.0 Hz, H-6'), 7.91(1H, d, J = 15.4 Hz, H-α), 7.83 (1H, d, J = 8.0 Hz, H-8), 7.50 (1H, t, J = 7.4 Hz, H-6), 7.44 (1H, d, J = 9.0 Hz, H-4), 7.34 (1H, t, J = 7.4 Hz, H-7), 7.07 (1H, d, J = 8.6 Hz, H-5'), 4.16 (2H, s, H-7'), 4.14 (2H, t, J = 6.6 Hz, H-1''), 3.23 (2H, br s, H-12), 2.84 (2H, br s, H-8'), 1.72 -1.81 (2H, m, H-2''),1.66 (4H, br s, H-9'/H-11), 1.29 (2H, br s, H-10'). 0.93 (3H, t, J = 6.6 Hz, H-3'') ^{13}C NMR (100 MHz, DMSO): δ 188.11 (C = O), 161.83 (C-4'), 156.97 (C-2), 136.52 (C-β), 135.12 (C-2'), 132.80 (C-1), 132.60 (C-3), 132.35 (C-6'), 129.85 (C-1'), 129.26 (C-8), 129.02 (C-9), 128.33 (C-6), 126.81 (C-α), 124.38 (C-7), 123.30 (C-5), 116.97 (C-3'), 116.75 (C-10), 116.27 (C-5'), 114.88 (C-4), 70.98 (C-1''), 54.04 (C-7'), 52.37 (C-8'/12), 22.76 (C-9'/10'/11), 21.62 (C-2''), 11.03 (C-3''). HR-APCI-MS: m/z 430.2362 [M + H]$^+$ (calcd for. $C_{28}H_{31}NO_3$ 429.2304)

E-1-[3-(piperidin-1-yl)methyl-4-hydroxyphenyl]-3-(2-(prop-2-yn-1-yloxy) naphthalen-1-yl)-2-propen-1-one (6)

Compound **4a** (0.23 g, 1 mmol) and **2b** (0.21 g, 1 mmol) was treated as described above. Chalcone **6** was obtained as a pale-yellow needle (0.40 g, 94%) R_f = 0.32 (EtOH: $CHCl_3$; 1:9), mp 203-205°C. IR: v_{max} cm^{-1} (KBr): 3433(OH), 3242 (C-H sp), 2938 (C-H sp^3), 2122 (C≡C), 1645 (C = O), 1602 (C = C) and 1297 (C-N). ^{1}HNMR (400 MHz, DMSO): δ 8.29 (1H, d, J = 2.0 Hz, H-2'), 8.27 (1H, d, J = 16.0 Hz, H-β), 8.20 (1H, d, J = 8.8 Hz, H-5), 8.07 (1H, dd, J = 8.5 and 2.0 Hz, H-6'), 8.06 (1H, d, J = 9.2 Hz, H-3), 7.97 (1H, d, J = 16.0 Hz, H-α), 7.95 (1H, d, J = 7.6 Hz, H-8), 7.61 (1H, t, J = 7.3 Hz, H-6), 7.59 (1H, d, J = 9.2 Hz, H-4), 7.46 (1H, t, J = 7.3 Hz, H-7), 7.17 (1H, d, J = 8.5 Hz, H-5'), 5.15 (2H, d, J = 2.4 Hz, H-1''),4.26 (2H, s, H-7'), 3.68 (1H, t, J = 2.2 Hz, H-3''), 3.31 (2H, br s, H-12), 2.92 (2H, br s, H-8'), 1.75 (4H, br s, H-9'/H-11), 1.38 (2H, br s, H-10').^{13}C NMR (100 MHz, DMSO): δ 187.98 (C = O), 161.94 (C-4'), 155.29 (C-2), 136.26 (C-β), 135.31 (C-2'), 132.59 (C-1), 132.44 (C-3), 132.10 (C-6'), 129.72 (C-1'), 129.49 (C-9), 129.22 (C-α), 128.35 (C-6), 127.63 (C-8), 124.77 (C-7), 123.61 (C-5), 117.95 (C-10), 116.90 (C-3'), 116.37 (C-5'), 115.25 (C-4), 79.77 (C-2''), 79.18 (C-3''), 57.27 (C-1''), 53.86 (C-7'), 52.25 (C-8'/12), 22.73 (C-9'/11), 21.66 (C-10'). HR-APCI-MS: m/z 426.2064 [M + H]$^+$ (calcd for. $C_{28}H_{27}NO_3$ 425.1991)

E-1-[3-(piperidin-1-yl)methyl-4-hydroxyphenyl]-3-(2-(benzyloxy)naph thalen-1-yl) -2-propen-1-one (7)

Compound **4a** (0.23 g, 1 mmol) and **2c** (0.26 g, 1 mmol) was treated as described above. Chalcone **7** was obtained as a pale-yellow crystal (0.4 g,84%) with R_f = 0.35 (EtOH: $CHCl_3$; 1:9), mp 138-140°C. IR:v_{max} cm^{-1} (KBr): 3400 (OH), 3063 (C-H sp^2), 2937 (C-H sp^3), 1647 (C = O), 1604 (C = C) and 1269 (C-N). ^{1}HNMR (400 MHz, DMSO): δ 8.36 (1H, d, J = 15.8 Hz, H-β), 8.20 (1H, d, J = 8.4 Hz, H-5), 8.16 (1H, d, J = 2.0 Hz, H-2'), 8.06(1H, d, J = 9.2 Hz, H-3), 7.97 (1H, d, J = 15. 8 Hz, H-α), 7.94 (1H, d, J = 8.8 Hz, H-8), 7.67 (1H, d, J = 9.0 Hz, H-4), 7.57-7.63 (4H, m, H-6, H-6', H-3'', H-7''), 7.38-7.47 (4H, m, H-7, H-4'', H-5'', H-6''), 7.02 (1H, d, J = 8.8 Hz, H-5'), 5.43 (2H, s, H-1''), 4.21 (2H, s, H-7'), 2.97 (4H, br s, H-8', H-12), 1.75 (4H, br s, H-9'/H-11), 1.50 (2H, br s, H-10'). ^{13}C NMR (100 MHz, DMSO): δ 187.86 (C = O), 161.75 (C-4'), 156.83 (C-2), 137.16 (C-2''), 136.06 (C-β), 134.91 (C-2'), 132.93 (C-1), 132.54 (C-3), 132.16 (C-6'), 129.74 (C-1'), 129.30 (C-8), 129.18 (C-9), 129.10 (C-3'', C-7''), 128.74 (C-4'', C-6''), 128.67 (C-5''), 128.36 (C-6), 126.76 (C-α), 124.53 (C-7), 123.19 (C-5), 117.17 (C-3'), 116.77 (C-10), 116.06 (C-5'), 115.15 (C-4), 71.20 (C-1''), 54.02 (C-7'), 52.32 (C-8'/12), 22.78 (C-9'/11), 21.66 (C-10'). HR-APCI-MS: m/z 478.2377 [M + H]$^+$ (calcd for. $C_{32}H_{31}NO_3$ 477.2304).

E-1-[3-(pyrrolidin-1-yl)methyl-4-hydroxyphenyl]-3-(2-propoxynaph- thalen-1-yl) -2-propen-1-one (8)

Compound **4b** (0.22 g, 1 mmol) and **2a** (0.21 g, 1 mmol) was treated as described above. Chalcone **8** was obtained as a yellow crystal (0.38 g, 91%) with R_f = 0.33 (EtOH: $CHCl_3$; 1:9), m.p 213–215°C. IR: v_{max} cm^{-1} (KBr): 3432 (OH), 2945 (C-H sp^3), 1646 (C = O), 1602 (C = C) and 1279 (C-N).^{1}HNMR (400 MHz, MeOD): δ 8.55 (1H, d, J = 15.6 Hz, H-β), 8.26 (1H, d, J = 8.4 Hz, H-5), 8.19 (1H, d, J = 2.0 Hz, H-2'), 8.13 (1H, dd, J = 8.5 and 2.0 Hz, H-6'), 8.10 (1H, d, J = 15.6 Hz, H-α), 7.98 (1H, d, J = 9.2 Hz, H-3), 7.88 (1H, d, J = 8.0 Hz, H-8), 7.59 (1H, ddd, J = 8.4, 5.6, 1.2 Hz,H-6), 7.49 (1H, d, J = 9.2 Hz, H-4), 7.34 (1H, dd, J = 8.0, 1.0 Hz, H-7), 7.11 (1H, d, J = 8.5 Hz, H-5'), 4.47 (2H, s, H-7'), 4.28 (2H, t, J = 6.4 Hz, H-1''), 3.41 (4H, t, J = 6.4 Hz, H-8'/H-11), 2.13 (4H, quin, H-9'/H-10'), 1.94 -2.03 (2H, m, H-2''), 1.16 (3H, t, J = 7.6 Hz, H-3''). ^{13}C NMR (100 MHz, DMSO) δ 188.03 (C = O), 161.41 (C-4'), 156.96 (C-2), 136.49 (C-β), 134.27 (C-2'), 132.80 (C-1), 132.58 (C-3), 132.21(C-6'), 129.86 (C-1'), 129.27 (C-8), 129.01(C-9), 128.32 (C-6), 126.84 (C-α), 124.38 (C-7), 123.31 (C-5), 118.51 (C-3'), 116.71 (C-10), 116.23 (C-5'), 114.86 (C-4), 70.94 (C-1''), 53.50 (C-8'/11), 52.02 (C-7'), 22.98 (C-9'/10'), 22.77 (C-2''), 11.08 (C-3'').

E-1-[3-(pyrrolidin-1-yl) methyl-4-hydroxy phenyl]-3-(2-(prop-2-yn-1-yloxy) naphthalen-1-yl)-2-propen-1-one (9)

Compound **4b** (0.22 g, 1 mmol) and **2b** (0.21 g, 1 mmol) was treated as described above. Chalcone **9** was obtained as a bright-yellow needle (0.34 g, 83%), with R_f = 0.35 (EtOH: $CHCl_3$; 1:9), m.p 218-220°C. IR: v_{max} cm^{-1} (KBr): 3436 (OH), 3206 (C-H sp), 3000 (C-H

sp^2), 2923 (C-H sp^3), 2119 (C≡C), 1656 (C = O), 1605 (C = C) and 1266 (C-N), 1132 (C-O). ^{1}HNMR (400 MHz, DMSO): δ 8.18 (1H, d, J = 15.6 Hz, H-β), 8.17 (1H, d, J = 2.1 Hz, H-2$'$), 8.11 (1H, d, J = 8.4 Hz, H-5), 7.98 (1H, dd, J = 8.7 and 2.1 Hz, H-6$'$), 7.98 (1H, d, J = 9.0 Hz, H-3), 7.87 (1H, d, J = 15.6 Hz, H-α), 7.87 (1H, d, J = 8.0 Hz, H-8), 7.52 (1H, ddd, J = 8.4, 5.2, 1.2 Hz, H-6), 7.51 (1H, d, J = 9.0 Hz, H-4), 7.38 (1H, dd, J = 8.0, 0.8 Hz, H-7), 7.07 (1H, d, J = 8.7 Hz, H-5$'$), 5.15 (2H, d, J = 2.0 Hz, H-1$''$),4.26 (2H, s, H-7$'$), 3.68 (1H, t, J = 2.4 Hz, H-3$''$), 3.16 (4H, br s, H-8$'$/ H-10$'$), 1.84 (4H, br s, H-9$'$/ H-11). ^{13}C NMR (100 MHz, DMSO): δ 187.90 (C = O), 161.45 (C-4$'$), 155.25 (C-2), 136.30 (C-β), 134.34 (C-2$'$), 132.54 (C-1), 132.37 (C-3), 132.14 (C-6$'$), 129.72 (C-1$'$), 129.46 (C-9), 129.24 (C-α), 128.37 (C-6), 127.55 (C-8), 124.79 (C-7), 123.58 (C-5), 118.54 (C-10), 117.85 (C-3$'$), 116.26 (C-5$'$), 115.18 (C-4), 79.76 (C-2$''$), 79.26 (C-3$''$), 57.20 (C-1$''$), 53.49 (C-8$'$/11), 51.94 (C-7$'$), 22.93 (C-9$'$/10$'$). HR-APCI-MS: m/z 412.1907 [M + H]$^+$ (calcd for. $C_{27}H_{25}NO_3$ 411.1834)

E-1-[3-(pyrrolidin-1-yl)methyl-4-hydroxy phenyl]-3-(2-(benzyloxy) naphthalen-1-yl)-2-propen-1-one (10)

Compound **4b** (0.22 g, 1 mmol) and **2c** (0.26 g, 1 mmol) was treated as described above. The product **10** was obtained as a light-yellow amorphous powder (0.45 g, 97%) with R_f = 0.35 (EtOH: CHCl$_3$; 1:9), mp 206-208°C. IR: v_{max} cm^{-1} (KBr): 3425 (OH), 2992 (C-H sp^2), 2922 (C-H sp^3), 1635 (C = O), 1593 (C = C) and 1289 (C-N), 1117 (C-O). ^{1}HNMR (400 MHz, DMSO): δ 8.38 (1H, d, J = 15.6 Hz, H-β), 8.22 (1H, d, J = 8.8 Hz, H-5), 8.18 (1H, d, J = 2.0 Hz, H-2$'$), 8.07 (1H, d, J = 9.2 Hz, H-3), 7.99 (1H, d, J = 15.6 Hz, H-α), 7.94 (1H, d, J = 9.6 Hz, H-8), 7.68 (1H, d, J = 9.2 Hz, H-4), 7.58 -7.65 (4H, m, H-6, H-6$'$, H-3$''$, H-7$''$), 7.42 -7.48 (4H, m, H-7, H-4$''$, H-5$''$, H-6$''$), 7.07 (1H, d, J = 8.4 Hz, H-5$'$), 5.43 (2H, s, H-1$''$), 4.32 (2H, s, H-7$'$), 3.12 (4H, br s, H-8$'$, H-11), 1.99 (2H, br s, H-10$'$), 1.88 (2H, br s, H-9$'$).^{13}C NMR (100 MHz, DMSO): δ 187.91 (C = O), 161.31 (C-4$'$), 156.83 (C-2), 137.14 (C-2$''$), 136.09 (C-β), 134.13 (C-2$'$), 132.93 (C-1), 132.55 (C-3), 132.07 (C-6$'$), 129.78(C-1$'$), 129.29 (C-8), 129.17 (C-9), 129.09 (C-3$''$, C-7$''$), 128.73 (C-4$''$, C-6$''$), 128.68 (C-5$''$), 128.36 (C-6), 126.75 (C-α), 124.53 (C-7), 123.18 (C-5), 118.52 (C-3$'$), 116.78 (C-10), 116.06 (C-5$'$), 115.15 (C-4), 71.20 (C-1$''$), 53.46 (C-8$'$/11), 51.92 (C-7$'$), 22.95 (C-9$'$/10$'$). HR-APCI-MS: m/z 464.2017 [M + H]$^+$ (calcd for. $C_{31}H_{29}NO_3$ 463.2147).

E-1-[3-(morpholinomethyl)-4-hydroxy phenyl]-3-(2-propoxy-naphthalen-1-yl) -2-propen-1-one (11)

Compound **4c** (0.24 g, 1 mmol) and **2a** (0.21 g, 1 mmol) was treated as described above. The product **11** was obtained as a light orange crystal (0.38 g, 88%), with R_f = 0.55 (EtOH: CHCl$_3$; 1:9), m.p 221-223°C. IR: v_{max} cm^{-1} (KBr): 3433 (OH), 3071 (C-H sp^2), 2919 (C-H sp^3), 1655 (C = O), 1603 (C = C), 1271 (C-N) and 1133 (C-O).^{1}HNMR (400 MHz, DMSO): δ 8.34 (1H, d, J = 15.8 Hz, H-β), 8.27 (1H, d, J = 2.2 Hz, H-2$'$), 8.19 (1H,

d, J = 8.8 Hz, H-5), 8.05 (1H, dd, J = 8.6 and 2.2 Hz, H-6$'$), 8.04 (1H, d, J = 9.2 Hz, H-3), 8.00 (1H, d, J = 15.8 Hz, H-α), 7.93 (1H, d, J = 8.0 Hz, H-8), 7.60 (1H, t, J = 7.3 Hz, H-6), 7.54 (1H, d, J = 9.2 Hz, H-4), 7.43 (1H, t, J = 7.3 Hz, H-7), 7.17 (1H, d, J = 8.6 Hz, H-5$'$), 4.34 (2H, s, H-7$'$), 4.24 (2H, t, J = 6.4 Hz, H-1$''$), 3.41 (4H, t, J = 6.2 Hz, H-8$'$/H-11), 3.91 (2H, br s, H-9$'$or 10$'$), 3.75 (2H, br s, H-9$'$or 10$'$), 3.28 (2H, br s, H-8$'$ or 11), 3.17 (2H, br s, H-8$'$ or 11), 1.82-1.91 (2H, m, H-2$''$), 1.04 (3H, t, J = 7.6 Hz, H-3$''$). ^{13}C NMR (100 MHz, DMSO) δ 187.99 (C = O), 161.95 (C-4$'$), 156.96 (C-2), 136.52(C-β), 135.39 (C-2$'$), 132.77 (C-1), 132.58 (C-3), 132.39(C-6$'$), 129.78 (C-1$'$), 129.26 (C-8), 128.34 (C-6), 126.79 (C-α), 124.35 (C-7), 123.36 (C-9), 123.28 (C-5), 116.71 (C-3$'$), 116.52 (C-10), 116.29 (C-5$'$), 114.81 (C-4), 70.90 (C-1$''$), 63.57 (C-9$'$/10$'$), 54.19 (C-7$'$), 51.23 (C-8$'$/11), 22.77 (C-2$''$), 11.02 (C-3$''$). HR-APCI-MS: m/z 432.2098 [M + H]$^+$ (calcd for. $C_{27}H_{29}NO_4$ 431.2097).

E-1-[3-(morpholinomethyl)-4-hydroxyphenyl]-3-(2-(prop-2-yn-1-yloxy) naphthalen-1-yl)-2-propen-1-one (12)

Compound **4c** (0.24 g, 1 mmol) and **2b** (0.21 g, 1 mmol) was treated as described above. The product **12** was obtained as a bright yellow needle (0.39 g, 91%), with R_f = 0.52 (EtOH: CHCl$_3$; 1:9), m.p 225-227°C. IR: v_{max} cm^{-1} (KBr): 3430 (OH), 3255 (C-H sp), 3093 (C-H sp^2), 2920 (C-H sp^3), 2127 (C≡C), 1649 (C = O), 1603 (C = C) and 1272 (C-N), 1132 (C-O).^{1}HNMR (400 MHz, DMSO): δ 8.27 (1H, d, J = 16.0 Hz, H-β), 8.2 7 (1H, d, J = 2.0 Hz, H-2$'$), 8.19 (1H, d, J = 8.4 Hz, H-5), 8.05- 8.09 (1H, m, H-6$'$), 8.07 (1H, d, J = 9.2 Hz, H-3), 7.95 (1H, d, J = 16.0 Hz, H-α), 7. 95 (1H, d, J = 8.0 Hz, H-8), 7.61 (1H, t, J = 7.5 Hz, H-6), 7.59 (1H, d, J = 9.2 Hz, H-4), 7.46 (1H, t, J = 7.5 Hz, H-7), 7.14 (1H, d, J = 8.4 Hz, H-5$'$), 5.14 (2H, d, J = 2.4 Hz, H-1$''$), 4.34 (2H, s, H-7$'$), 3.91 (2H, br s, H-9$''$), 3.71 (2H, br s, H-10$'$), 3.67 (1H, t, J = 2.2 Hz, H-3$''$), 3.38 (2H, br s, H-8$'$ or 11), 3.16 (2H, br s, H-8$'$ or 11).^{13}C NMR (100 MHz, DMSO) δ 187.97 (C = O), 161.87 (C-4$'$), 155.27 (C-2), 136.33(C-β), 135.27 (C-2$'$), 132.64 (C-1), 132.57 (C-3), 132.14(C-6$'$), 129.79 (C-1$'$), 129.49 (C-8), 129.24 (C-6), 128.36 (C-α), 127.60 (C-7), 124.79 (C-9), 123.58 (C-5), 117.93 (C-3$'$), 116.59 (C-10), 116.32 (C-5$'$), 115.24 (C-4), 79.75 (C-2$''$), 79.18 (C-3$''$), 63.63 (C-9$'$/10$'$), 57.27 (C-1$''$), 54.38 (C-7$'$), 51.48 (C-8$'$/11). HR-APCI-MS: m/z 428.1761 [M + H]$^+$ (calcd for. $C_{27}H_{25}NO_4$ 427.1784).

E-1-[3-(morpholinomethyl)-4-hydroxyphenyl]-3-(2-(benzyloxy)naph-thalen-1-yl)-2-propen-1-one (13)

Compound **4c** (0.24 g, 1 mmol) and **2c** (0.26 g, 1 mmol) was treated as described above. The product **13** was obtained as a light-yellow needle (0.40 g, 84%) with R_f = 0.54 (EtOH: CHCl$_3$; 1:9), mp 205-208°C. IR: v_{max} cm^{-1} (KBr): 3431 (OH), 2972 (C-H sp^2), 2926 (C-H sp^3), 1664 (C = O), 1622 (C = C), 1274 (C-N) and 1128 (C-O). ^{1}HNMR (400 MHz, DMSO): δ 8.36 (1H, d, J = 15.8 Hz, H-β), 8.20 (1H, d, J = 8.4 Hz, H-5), 8.17 (1H, d, J = 2.4 Hz, H-2$'$), 8.05 (1H, d, J = 9.2 Hz, H-3), 7.97 (1H, d, J = 15.8 Hz, H-α), 7.94 (1H, d, J = 9.2 Hz, H-8), 7.66 (1H, d, J = 9.2 Hz, H-4), 7.56 -7.63 (4H, m, H-6, H-6$'$, H-3$''$, H-7$''$), 7.39 -7.46

(4H, m, H-7, H-4″, H-5″, H-6″), 7.05 (1H, d, $J = 8.8$ Hz, H-5′), 5.07 (2H, s, H-1″), 4.13 (2H, s, H-7′), 3.65 (4H, s, H-9′/10′), 3.05 (4H, br s, H-8′/11). ^{13}C NMR (100 MHz, DMSO): δ 187.94 (C = O), 161. 33 (C-4′), 156.86 (C-2), 137.17 (C-2″), 136.11 (C-β), 134.16 (C-2′), 132.95 (C-1), 132.58 (C-3), 132.09 (C-6′), 129.81(C-1′), 129.32 (C-8), 129.20 (C-9), 129.11 (C-3″, C-7″), 128.75 (C-4″, C-6″), 128.71 (C-5″), 128.39 (C-6), 126.77 (C-α), 124.56 (C-7), 123.21 (C-5), 118.54 (C-3′), 116.81 (C-10), 116.09 (C-5′), 115.17 (C-4), 71.24 (C-1″), 63.62 (C-9′/10′), 54.24 (C-7′), 51.92 (C-8′/11). HR-APCI-MS: m/z 480.2169 [M + H]$^+$ (calcd for. $C_{31}H_{29}NO_4$ 479.2097).

E-1-[3-(diethylamino)methyl-4-hydroxy phenyl]-3-(2-propoxy-naph-thalen-1-yl)-2-propen-1-one (14)

Compound **4d** (0.22 g, 1 mmol) and **2a** (0.21 g, 1 mmol) was treated as described above. The product **14** was obtained as a dark yellow amorphous powder (0.35 g, 84%), with R$_f$ = 0.45 (EtOH: CHCl$_3$; 1:9), m.p 188-191°C. IR: v_{max} cm^{-1} (KBr): 3433 (OH), 2941 (C-H sp^3), 1642 (C = O), 1602 (C = C), 1278 (C-N) and 1093 (C-O). ^{1}HNMR (400 MHz, DMSO): δ 8.34 (1H, d, $J = 16.0$ Hz, H-β), 8.25 (1H, d, $J = 1.6$ Hz, H-2′), 8.19 (1H, d, $J = 8.4$ Hz, H-5), 8.02- 8.05 (1H, m, H-6′), 8.03 (1H, d, $J = 9.2$ Hz, H-3), 8.01 (1H, d, $J = 16.0$ Hz, H-α), 7. 93 (1H, d, $J = 8.0$ Hz, H-8), 7.59 (1H, t, $J = 7.6$ Hz, H-6), 7.53 (1H, d, $J = 9.2$ Hz, H-4), 7.43 (1H, t, $J = 7.6$ Hz, H-7), 7.19 (1H, d, $J = 8.8$ Hz, H-5′), 4.29 (2H, s, H-7′), 4.23 (2H, t, $J = 6.4$ Hz, H-1″), 3.10 (4H, q, $J = 7.2$ Hz, 2∗CH$_2$), 1.82-1.91 (2H, m, H-2″), 1.26 (6H, t, $J = 7.2$ Hz, 2∗CH$_3$), 1.03 (3H, t, $J = 7.4$ Hz, H-3″). ^{13}C NMR (100 MHz, DMSO) δ 187.98 (C = O), 161.87 (C-4′), 156.96 (C-2), 136.44(C-β), 134.75 (C-2′), 132.80 (C-1), 132.56 (C-3), 132.17(C-6′), 129.78 (C-1′), 129.25 (C-8), 128.99 (C-6), 128.31 (C- α), 126.75 (C-7), 124.34 (C-9), 123.34 (C-5), 117.48 (C-3′), 116.67(C-10), 116.32 (C-5′), 114.80 (C-4), 70.88 (C-1″), 49.99 (C-7′), 46.70 (2∗CH$_2$), 22.76(C-2″), 11.06(C-3″), 8.95 (2∗CH$_3$). HR-APCI-MS: m/z 418.2359 [M + H]$^+$ (calcd for. $C_{27}H_{31}NO_3$ 417.2304).

E-1-[3-(diethylamino)methyl-4-hydroxy phenyl]-3-(2-(prop-2-yn-1-yloxy) naphthalen-1-yl)-2-propen-1-one (15)

Compound **4d** (0.22 g, 1 mmol) and **2b** (0.21 g, 1 mmol) was treated as described above. The product **15** was obtained as an orange amorphous powder (0.4 g, 96%), with R$_f$ = 0.35 (EtOH: CHCl$_3$; 1:9), m.p 140–143°C. IR: v_{max} cm^{-1} (KBr): 3396 (OH), 3237 (C-H sp), 3062 (C-H sp^2), 2929 (C-H sp^3), 2124 (C≡C), 1640 (C = O), 1603 (C = C) and 1269 (C-N), 1138 (C-O).^{1}HNMR (400 MHz, DMSO): δ 8.26 (1H, d, $J = 15.6$ Hz, H-β), 8.21 (1H, d, $J = 1.6$ Hz, H-2′), 8.19 (1H, d, $J = 8.4$ Hz, H-5), 8.05- 8.09 (1H, m, H-6′), 8.06 (1H, d, $J = 9.2$ Hz, H-3), 7.96 (1H, d, $J = 15.6$ Hz, H-α), 7. 95 (1H, d, $J = 8.4$ Hz, H-8), 7.60 (1H, t, $J = 7.4$ Hz, H-6), 7.58 (1H, d, $J = 9.2$ Hz, H-4), 7.46 (1H, t, $J = 7.4$ Hz, H-7), 7.14 (1H, d, $J = 8.8$ Hz, H-5′), 5.12 (2H, d, $J = 2.2$ Hz, H-1″), 4.29 (2H, s, H-7′), 3.67 (1H, t, $J = 2.2$ Hz, H-3″), 3.09 (4H, q, $J = 7.2$ Hz, 2∗CH$_2$), 1.24 (6H, t, $J = 7.2$ Hz, 2∗CH$_3$).[13]C

NMR (100 MHz, DMSO) δ 187.91 (C = O), 161.88 (C-4′), 155.30 (C-2), 136.26(C-β), 134.79 (C-2′), 132.57 (C-1), 132.36 (C-3), 132.15(C-6′), 129.68 (C-1′), 129.45 (C-8), 129.24 (C-6), 128.37 (C- α), 127.51 (C-7), 124.77 (C-9), 123.60 (C-5), 117.82 (C-3′), 117.56 (C-10), 116.35 (C-5′), 115.18 (C-4), 79.77 (C-2″), 79.26 (C-3″), 57.20 (C-1″), 50.03 (C-7′), 46.70 (2∗CH$_2$), 8.97 (2∗CH$_3$). HR-APCI-MS: m/z 414.2064 [M + H]$^+$ (calcd for. $C_{27}H_{27}NO_3$ 413.1991).

E-1-[3-(diethylamino)methyl-4-hydroxyphenyl]-3-(2-(benzyloxy)naph-thalen-1-yl)-2-propen-1-one (16)

Compound **4d** (0.22 g, 1 mmol) and **2c** (0.26 g, 1 mmol) was treated as described above. The crude product **16** was obtained as a yellow amorphous powder (0.43 g, 92%), with R$_f$ = 0.38 (EtOH: CHCl$_3$; 1:9), m.p 146-148°C. IR: v_{max} cm^{-1} (KBr): 3386 (OH), 3060 (C-H sp^2), 2933 (C-H sp^3), 1651 (C = O), 1607 (C = C) and 1267 (C-N), 1139 (C-O). ^{1}HNMR (400 MHz, DMSO): δ 11.58 (1H, s, OH), 8.38 (1H, d, $J = 15.4$ Hz, H-β), 8.21 (1H, d, $J = 8.8$ Hz, H-5), 8.20 (1H, d, $J = 2.0$ Hz, H-2′), 8.06 (1H, d, $J = 9.0$ Hz, H-3), 8.04 (1H, d, $J = 15.4$ Hz, H-α), 7.95 (1H, d, $J = 8.0$ Hz, H-8), 7.67 (1H, d, $J = 9.0$ Hz, H-4), 7.58 -7.63 (4H, m, H-6, H-6′, H-3″, H-7″), 7.42 -7.47 (4H, m, H-7, H-4″, H-5″, H-6″), 7.11 (1H, d, $J = 8.4$ Hz, H-5′), 5.44 (2H, s, H-1″), 4.25 (2H, s, H-7′), 3.06 (4H, q, $J = 7.2$ Hz, 2∗CH$_2$), 1.25 (6H, t, $J = 7.0$ Hz, 2∗CH$_3$). ^{13}C NMR (100 MHz, DMSO): δ 187.81 (C = O), 161.71 (C-4′), 156.85 (C-2), 137.16 (C-2″), 136.05 (C-β), 134.54 (C-2′), 132.92 (C-1), 132.58 (C-3), 132.10 (C-6′), 129.70 (C-1′), 129.31 (C-8), 129.15 (C-9), 129.10 (C-3″, C-7″), 128.76 (C-4″, C-6″), 128.70 (C-5″), 128.38 (C-6), 126.67 (C-α), 124.52 (C-7), 123.20 (C-5), 117.65 (C-3′), 116.68 (C-10), 116.08 (C-5′), 115.10 (C-4), 71.13 (C-1″), 50.02 (C-7′), 46.72 (2∗CH$_2$), 8.93(2∗CH$_3$). HR-APCI-MS: m/z 466.2335 [M + H]$^+$ (calcd for. $C_{31}H_{31}NO_3$ 465.2304).

4.2. Bioactivities analysis

4.2.1. DPPH radical scavenging activity

The antioxidant evaluation was performed against 2,2-diphenyl-1-picrylhydrazyl (DPPH) free radical based on the method described by Hamad *et. al.* [46]. Briefly, a stock solution of chalcones **5–16** in methanol were diluted to final concentrations from 1280 to 10 μg/ml. An aliquot of 40 μL of each test sample (8 serial dilutions) was mixed with 160 μL of freshly prepared methanolic solution of (DPPH) radical 100 μM and kept in the dark. After 30 min of incubation, the decrease in absorbance at 517 nm was determined. The absorbance of the DPPH radical without antioxidant (blank) and the reference compound ascorbic acid were also measured. All the determinations were performed in three replicates and averaged. The percentage inhibition of the DPPH radical was calculated according to the formula:

$$\text{Percentage Inhibition (\%)} = \frac{(A_{blank} - A_{sample})}{A_{blank}} \times 100$$

Where A_{blank} = absorbance of the blank solution (containing DPPH solution without sample) and A_{sample} = absorbance of a sample solution. The concentration affording 50% inhibition (IC_{50}) values were calculated by plotting scavenging percentages against concentrations of the sample.

4.2.2. Acetylcholinesterase inhibitory assay

The acetylcholinesterase inhibitory activity of chalcones **5–16** were determined by Ellman's microplate assay described by Koay *et al.* [44]. 140 µl of 0.1 M sodium phosphate buffer (pH 8) was first added followed by 20 µl of each test sample (in 10% methanol) and 20 µl of 0.09 unit/ml AChE. After pre-incubation at room temperature, 10 µl of 10 mM 5,5′-dithiobis (2- nitrobenzoic acid) DTNB was added into each well followed by 10 µl of 14 mM acetylthiocholine iodide as substrate. The absorbance of the coloured product was measured using a microplate reader at 412 nm following 30 min incubation. Donepezil was used as a positive control. Percentage inhibition was calculated using the following formula for different eight concentrations:

$$\text{Percentage inhibition} = \frac{(\text{absorbance of control} - \text{absorbance of sample})}{\text{absorbance of control}} \times 100$$

Three replicates of each sample were used for statistical analysis with values reported as mean ± S.D. Standard curves were generated and calculations of the 50% inhibitory concentration (IC_{50}) values were done using GraphPad Prism for Windows (version 8.3.0) software.

4.3. In silico predictions of drug-likeness; pharmacokinetic; toxicity and target predictions

The *in silico* studies of the synthesized chalcones were predicted using online web tools: http://www.swissadme.ch [32]; https://www.molinspiration.com/ and http://lmmd.ecust.edu.cn/admetsar2/ [47].

4.4. Molecular docking

Docking study was carried out using AUTODOCK 4.2 as a programme to screen the binding affinity of all chalcones on the Torpedo california acetylcholinesterase (TcAChE) [48]. The X-ray crystal structure of the acetylcholinesterase complexed with donepezil E20 (PDB code: 1EVE) was obtained from the Protein Data Bank (https://www.rcsb.org/structure/1eve). All ligands and water molecules were removed from the retrieved protein using Discovery Studio Visualizer v17.2.0.16349 [49]. Docking calculations were carried out using the Lamarckian genetic algorithm (LGA), and all parameters were the same for each docking. The grid box size was set at 40,40, 40 A°, while the centre of the grid box was set at 2.023(x), 63.295(y) and 67.062(z). the spacing between the grid points was 0.375A°. The 2D structures of the novel chalcones were sketched in ChemBio Draw Ultra 12.0, which were then converted to three-dimensional structures in ChemBio3D Ultra 12.0. and then the structures geometry optimization was performed using the PM3 process for the MOPAC Ultra 2009 programme to build the 3D pdbqt format.[50] The chalcones-protein interactions for the most stable binding modes of each chalcone in the active site of TcAChE were analyzed and visualized in Two-dimensional (2D) diagrams using Discovery Studio Visualizer.

Disclosure statement

No potential conflict of interest was reported by the author(s).

ORCID

Ghadah Aljohani http://orcid.org/0000-0003-0406-416X
Adeeb Al-Sheikh Ali http://orcid.org/0000-0001-8964-1733
Shaya Y. Alraqa http://orcid.org/0000-0002-2622-581X
Syazwani Itri Amran http://orcid.org/0000-0002-5873-5291
Norazah Basar http://orcid.org/0000-0002-6195-0419

References

[1] Massoulié J, Pezzementi L, Bon S, et al. Molecular and cellular biology of cholinesterases. Prog Neurobiol. 1993;41:31–91. doi:10.1016/0301-0082(93)90040-Y.

[2] Mishra P, Kumar A, Panda G. Anti-cholinesterase hybrids as multi-target-directed ligands against Alzheimer's disease (1998–2018). Bioorg Med Chem. 2019;27:895–930. doi:10.1016/j.bmc.2019.01.025.

[3] Dvir H, Silman I, Harel M, et al. Acetylcholinesterase: from 3D structure to function. Chem Biol Interact. 2010;187:10–22. doi:10.1016/j.cbi.2010.01.042.

[4] Saxena A, Redman AMG, Jiang X, et al. Differences in active site gorge dimensions of cholinesterases revealed by binding of inhibitors to human butyrylcholinesterase. Biochemistry. 1997;36:14642–14651. doi:10.1021/bi971425+.

[5] Kovarik Z, Bosak A, Šinko G, et al. Exploring the active sites of cholinesterases by inhibition with bambuterol and haloxon. Croat Chem Acta. 2003;76:63–67.

[6] Liston DR, Nielsen JA, Villalobos A, et al. Pharmacology of selective acetylcholinesterase inhibitors: implications for use in Alzheimer's disease. Eur J Pharmacol. 2004;486:9–17. doi:10.1016/j.ejphar.2003.11.080.

[7] Martinez A, Castro A. Novel cholinesterase inhibitors as future effective drugs for the treatment of Alzheimer's disease. Expert Opin Investig Drugs. 2006;15:1–12. doi:10.1517/13543784.15.1.1.

[8] Spencer CM, Noble S. Rivastigmine. A review of its use in Alzheimer's disease. Drugs and Aging. 1998;13:391–411. doi:10.2165/00002512-199813050-00005.

[9] Dooley M, Lamb HM. Donepezil. A review of its use in Alzheimer's disease. Drugs and Aging. 2000;16:199–226. doi:10.2165/00002512-200016030-00005.

[10] Maelicke A, Samochocki M, Jostock R, et al. Allosteric sensitization of nicotinic receptors by galantamine, a new treatment strategy for Alzheimer's disease. Biol Psychiatry. 2001;49:279–288. doi:10.1016/S0006-3223(00)01109-4.

[11] Watkins PB, Zimmerman HJ, Knapp MJ, et al. Hepatotoxic effects of tacrine administration in patients with Alzheimer's disease. The Journal of the American Medical Association. 1994;271:992–998.

[12] Dhanjal JK, Sharma S, Grover A, et al. Use of ligand-based pharmacophore modeling and docking approach to find novel acetylcholinesterase inhibitors for treating Alzheimer's. Biomed Pharmacother. 2015;71:146–152. doi:10.1016/j.biopha.2015.02.010.

[13] Wang L, Wang Y, Tian Y, et al. Design, synthesis, biological evaluation, and molecular modeling studies of chalcone-rivastigmine hybrids as cholinesterase inhibitors. Bioorg Med Chem. 2017;25:360–371. doi:10.1016/j.bmc.2016.11.002.

[14] Berar U. ChemInform abstract: chalcones: compounds possessing a diversity in applications. ChemInform. 2013;44:209–221. doi:10.1002/chin.201318260.

[15] Matos MJ, Vazquez-Rodriguez S, Uriarte E, et al. Potential pharmacological uses of chalcones: a patent review (from June 2011-2014). Expert Opin Ther Pat. 2015;25:351–366. doi:10.1517/13543776.2014.995627.

[16] Chavan BB, Gadekar AS, Mehta PP, et al. Synthesis and medicinal significance of chalcones-a review. Asian Journel of Biomedical and Pharmaceutical Sciences. 2016;6:1–7. www.jbiopharm.com.

[17] Zhuang C, Zhang W, Sheng C, et al. Chalcone: a privileged structure in medicinal chemistry. Chem Rev. 2017;117:7762–7810. doi:10.1021/acs.chemrev.7b00020.

[18] Chen YP, Zhang ZY, Li YP, et al. Syntheses and evaluation of novel isoliquiritigenin derivatives as potential dual inhibitors for amyloid-beta aggregation and 5-lipoxygenase. Eur J Med Chem. 2013;66:22–31. doi:10.1016/j.ejmech.2013.05.015.

[19] Liu H-R, Zhou C, Fan H-Q, et al. Novel potent and selective acetylcholinesterase inhibitors as potential drugs for the treatment of Alzheimer's disease: synthesis, pharmacological evaluation, and molecular modeling of aminoalkyl-substituted fluoro-chalcones derivatives. Chem Biol Drug Des. 2015;86:517–522. doi:10.1111/cbdd.12514.

[20] Liu HR, Huang XQ, Lou DH, et al. Synthesis and acetylcholinesterase inhibitory activity of Mannich base derivatives flavokawain B. Bioorg Med Chem Lett. 2014;24:4749–4753. doi:10.1016/j.bmcl.2014.07.087.

[21] Liu H, Liu X, Fan H, et al. Design, synthesis and pharmacological evaluation of chalcone derivatives as acetylcholinesterase inhibitors. Bioorg Med Chem. 2014;22:6124–6133. doi:10.1016/j.bmc.2014.08.033.

[22] Liu H, Huang X, Lou D, et al. Synthesis and acetylcholinesterase inhibitory activity of Mannich base derivatives flavokawain B. Bioorg Med Chem Lett. 2014;24:4749–4753. doi:10.1016/j.bmcl.2014.07.087.

[23] Park DH, Venkatesan J, Kim SK, et al. Antioxidant properties of Mannich bases. Bioorg Med Chem Lett. 2012;22:6362–6367. doi:10.1016/j.bmcl.2012.08.080.

[24] Roman G. Mannich bases in medicinal chemistry and drug design. Eur J Med Chem. 2015;89:743–816. doi:10.1016/j.ejmech.2014.10.076.

[25] Li Y, Qiang X, Luo L, et al. Aurone Mannich base derivatives as promising multifunctional agents with acetylcholinesterase inhibition, anti-β-amyloid aggregation and neuroprotective properties for the treatment of Alzheimer's disease. Eur J Med Chem. 2017;126:762–775. doi:10.1016/j.ejmech.2016.12.009.

[26] Zhang X, Song Q, Cao Z, et al. Design, synthesis and evaluation of chalcone Mannich base derivatives as multifunctional agents for the potential treatment of Alzheimer's disease. Bioorg Chem. 2019;87:395–408. doi:10.1016/j.bioorg.2019.03.043.

[27] Tian C, Qiang X, Song Q, et al. Flurbiprofen-chalcone hybrid Mannich base derivatives as balanced multifunctional agents against Alzheimer's disease: design, synthesis and biological evaluation. Bioorg Chem. 2020;94:103477), doi:10.1016/j.bioorg.2019.103477.

[28] Young DC. Computational drug design: A guide for Computational and Medicinal chemists. Hoboken (NJ): John Wiley & Sons, Inc; 2009.doi:10.1002/9780470451854

[29] Liu H, Liu X, Fan H, et al. Design, synthesis and pharmacological evaluation of chalcone derivatives as acetylcholinesterase inhibitors. Bioorg Med Chem. 2014;22:6124–6133. doi:10.1016/j.bmc.2014.08.033.

[30] Cao YQ, Xi Y, Teng XY, et al. Alkoxy substituted D-π-A dimethyl-4-pyrone derivatives: aggregation induced emission enhancement, mechanochromic and solvatochromic properties. Dyes Pigm. 2017;137:75–83. doi:10.1016/j.dyepig.2016.09.063.

[31] Aljohani G, Lentz D, Said MA, et al. Crystal structure of 2-(prop-2-yn-1-yloxy)-1-naphthaldehyde, C14H10O2, zeitschrift Für kristallographie. New Crystal Structures. 2019;234:977–978. doi:10.1515/ncrs-2019-0195.

[32] Quideau S, Pouységu L, Oxoby M, et al. 2-Alkoxyarenol-derived orthoquinols in carbon-oxygen, carbon-nitrogen and carbon-carbon bond-forming reactions. Tetrahedron. 2001;57:319–329. doi:10.1016/S0040-4020(00)00939-X.

[33] Aljohani G, Said MA, Lentz D, et al. Microwave-assisted synthesis of mono- and disubstituted 4-hydroxyacetophenone derivatives via mannich reaction: synthesis, XRD and HS-analysis. Molecules. 2019;24:590, doi:10.3390/molecules24030590.

[34] Cavalli A, Bolognesi ML, Minarini A, et al. Multi-target-Directed ligands To combat neurodegenerative diseases. J Med Chem. 2008;51:347–372. doi:10.1021/jm7009364.

[35] Moroy G, Martiny VY, Vayer P, et al. Toward in silico structure-based ADMET prediction in drug discovery. Drug Discov Today. 2012;17:44–55. doi:10.1016/j.drudis.2011.10.023.

[36] Daina A, Michielin O, Zoete V. SwissADME: A free web tool to evaluate pharmacokinetics, drug-likeness and medicinal chemistry friendliness of small molecules. Sci Rep. 2017;7; doi:10.1038/srep42717.

[37] Tian S, Wang J, Li Y, et al. The application of in silico drug-likeness predictions in pharmaceutical research. Adv Drug Deliv Rev. 2015;86:2–10. doi:10.1016/j.addr.2015.01.009.

[38] Lipinski CA, Lombardo F, Dominy BW, et al. Experimental and computational approaches to estimate solubility and permeability in drug discovery and development settings. Adv Drug Deliv Rev. 2012;64:4–17. doi:10.1016/j.addr.2012.09.019.

[39] Ertl P, Rohde B, Selzer P. Fast calculation of molecular polar surface area as a sum of fragment-based contributions and its application to the prediction of drug transport properties. J Med Chem. 2000;43:3714–3717. doi:10.1021/jm000942e.

[40] Martin YC. A bioavailability score. J Med Chem. 2005;48: 3164–3170. doi:10.1021/jm0492002.

[41] Daina A, Michielin O, Zoete V. Swisstargetprediction: updated data and new features for efficient prediction of protein targets of small molecules. Nucleic Acids Res. 2019;47:W357–W3664. doi:10.1093/nar/gkz382.

[42] Leong SW, Abas F, Lam KW, et al. 2-Benzoyl-6-benzylidenecyclohexanone analogs as potent dual inhibitors of acetylcholinesterase and butyrylcholinesterase. Bioorg Med Chem. 2016;24:3742–3751. doi:10.1016/j.bmc.2016.06.016.

[43] Ko FN, Cheng ZJ, Lin CN, et al. Scavenger and antioxidant properties of prenylflavones isolated from artocarpus heterophyllus. Free Radical Biol Med. 1998;25:160–168. doi:10.1016/S0891-5849(98)00031-8.

[44] Koay Y-H, Basiri A, Murugaiyah V, et al. Isocorilagin, a cholinesterase inhibitor from phyllanthus niruri. Nat Prod Commun. 2014;9:515–517. doi:10.1177/1934578X1400900423.

[45] Aljohani G, Ali AA-S, Said MA, et al. 2-Benzyloxynaphthalene aminoalkylated chalcone designed as acetylcholinesterase inhibitor: structural characterisation, in vitro biological activity and molecular docking studies. J Mol Struct. 2020;1222:128898), doi:10.1016/j.molstruc.2020.128898.

[46] Hamad I, AbdElgawad H, al Jaouni S, et al. Metabolic analysis of various date palm fruit (phoenix dactylifera L.) cultivars from Saudi Arabia to assess their nutritional quality. Molecules. 2015;20:13620–13641. doi:10.3390/molecules200813620.

[47] Yang H, Lou C, Sun L, et al. AdmetSAR 2.0: Webservice for prediction and optimization of chemical ADMET properties. Bioinformatics. 2019;35:1067–1069. doi:10.1093/bioinformatics/bty707.

[48] Morris GM, Ruth H, Lindstrom W, et al. Autodock4 and AutoDockTools4: automated docking with selective receptor flexibility. J Comput Chem. 2009;30:2785–2791. doi:10.1002/jcc.21256.

[49] Biovia DS. Discovery studio modeling environment, (2017).

[50] Stewart JJP. MOPAC2009 Stewart Computational Chemistry, Version 10.124L, (2009). http://openmopac.net/.